A new ornithomimid dinosaur with gregarious habits from the Late Cretaceous of China

YOSHITSUGU KOBAYASHI and JUN-CHANG LÜ

At least fourteen ornithomimid skeletons were recovered from the Upper Cretaceous Ulansuhai Formation in Nei Mongol (Inner Mongolia) Autonomous Region of China. They are assigned to a new genus and species, *Sinornithomimus dongi*. The anatomy of the species is described. Comparative and phylogenetic studies of ornithomimosaurs prove that these skeletons represent a new taxon that is more derived than *Archaeornithomimus* and more basal than the clade of [(*Anserimimus* + *Gallimimus*) + [*Struthiomimus* + (*Dromiceiomimus* + *Ornithomimus*)]]. The phylogenetic analysis suggests that the structure of the hand is similar to *Archaeornithomimus* and represents an intermediate condition between the primitive (*Harpymimus*) and the derived (*Anserimimus*, *Gallimimus*, *Struthiomimus*, *Dromiceiomimus*, and *Ornithomimus*) conditions. The monophyly of Ornithomimidae is supported by a single synapomorphy (arctometatarsalian condition) in this analysis, indicating that the family is not as strongly supported as previously suggested. The analysis also implies that the shape of the rhamphotheca in North American taxa may have been different from that in Asian taxa. Previous study suggests herbivorous habits of this dinosaur based on characteristics of the gastroliths. The skeletons of *Sinornithomimus* were collected from a single monospecific bonebed with a high ratio of juvenile individuals (11 of the 14), suggesting gregarious behavior for protection from predators. The abundance of juveniles indicates high mortality of juveniles or a catastrophic mass mortality of a population with a high proportion of juveniles. An increase in the relative ratio of the tibia to femur through the ontogeny of *Sinornithomimus* suggests higher cursoriality in adult individuals than in juveniles.

Key words: Dinosauria, Theropoda, Ornithomimosauria, Ornithomimidae, Late Cretaceous, China.

Yoshitsugu Kobayashi [ykobayashi@dinosaur.pref.fukui.jp], Fukui Prefectural Dinosaur Museum, Katsuyama, Fukui 911-8601 JAPAN;
Jun-Chang Lü [junchang@mail.smu.edu], Department of Geological Sciences, Southern Methodist University, Dallas Texas 75275 USA.

Introduction

The People's Republic of China is known to be one of the richest countries in dinosaur fossils and has numerous exposures of Upper Cretaceous sediments. Remains of ornithomimosaurian dinosaurs have been commonly discovered in Upper Cretaceous sediments of North America and Mongolia. However, well-preserved ornithomimosaur skeletons are hardly known from China. The only previously known genus from China is *Archaeornithomimus asiaticus* (Gilmore, 1933), which is based on disarticulated skeletons with partially articulated vertebral series (Smith and Galton 1990).

In the summer of 1997, the Mongol Highland International Dinosaur Project (MHIDP) with researchers from Japan, China, and Mongolia (Kobayashi et al. 1999) found at least fourteen ornithomimosaur skeletons in the Upper Cretaceous Ulansuhai Formation in Alashanzuo Banner, Nei Mongol (Inner Mongolia) Autonomous Region, in the northern part of China (Fig. 1). Nine of these skeletons are nearly complete and relatively uncrushed. All were discovered in a monospecific bonebed in an area of 2 m by 5 m (Figs. 2, 3). Kobayashi et al. (2001) suggested that the Ulan Suhai

ornithomimosaur belongs to the Ornithomimidae and can be distinguished from other ornithomimids as a new taxon.

Late Cretaceous Ornithomimosauria from eastern Asia and North America, excluding *Garudimimus brevipes* Barsbold, 1981 from Mongolia, form the monophyletic Ornithomimidae (Barsbold and Osmólska 1990; Osmólska 1997; Norell et al. 2002; Makovicky et al. in press). All members of Ornithomimidae have edentulous jaws and long necks, as well as long forelimbs and hindlimbs. Among the six genera and eight species in the family, three genera and species are known from Asia: *Gallimimus bullatus* Osmólska, Roniewicz, and Barsbold, 1972 (Mongolia), *Anserimimus planinychus* Barsbold, 1988 (Mongolia), and *Archaeornithomimus asiaticus*. The Asian ornithomimids, especially *Gallimimus bullatus* (Osmólska et al. 1972) and *Archaeornithomimus asiaticus* (Smith and Galton 1990), are well described. Limb proportions of these animals were compared with North American taxa (*Ornithomimus* Marsh, 1890, *Dromiceiomimus* Russell, 1972, and *Struthiomimus* Osborn, 1916) by Nicholls and Russell (1981, 1985). However, the phylogenetic relationships within Ornithomimidae remain unresolved because many ornithomimosaur specimens are poorly preserved or crushed. The Ulan Suhai specimens are the first

Acta Palaeontol. Pol. 48 (2): 235–259, 2003

http://app.pan.pl/acta48/app48-235.pdf

ornithomimids discovered from a bonebed of well-preserved, articulated skeletons. The anatomical study of these specimens helps to resolve the relationships of ornithomimids.

Geology

The Ulan Suhai locality is near Ulan Suhai, Alashanzuo Banner, near the boundary of China with Mongolia (Fig. 1). The Upper Cretaceous Ulansuhai Formation (report of Bureau of Geology and Mineral Resources of Nei Mongol Autonomous Region 1991) crops out in the western part of the Nei Mongol Autonomous Region (also called the North Alashan Geological Region). It consists mainly of reddish sandstones and mudstones. The facies of the type section consists of gray conglomerates (2 meters thick), yellowish-gray mudstone (5 meters thick), light gray sandstone (7 meters thick), reddish sandstone containing *Protoceratops* (17 meters thick), and reddish mudstone with inclusions of gray sandstone and gypsum (at least 62 meters thick). The formation unconformably overlies the Lower Cretaceous Suhongtu or Bayingebi formations.

Basalts from the Suhongtu Formation were dated from 146 to 92 Ma by the whole-rock K-Ar dating method, indicating that the Ulansuhai Formation is at least younger than 92 Ma (report of Bureau of Geology and Mineral Resources of Nei Mongol Autonomous Region 1991). The faunal assemblage including *Protoceratops* sp. supports a Late Cretaceous age. Remains of *Bactrosaurus*, a tyrannosaurid, and an ankylosaur were reported from the North Alashan Geological Region, but the stratigraphic position of these specimens is not determined. At the Ulan Suhai locality, a surangular of an iguanodontian dinosaur was discovered just below the ornithomimid horizon. It has a surangular foramen as seen in non-hadrosaurid iguanodontians. This indicates that the surangular does not belong to *Bactrosaurus* (Godefroit et al. 1998), but is closer to basal hadrosaurids (Head 2001), and suggests that the age is possibly early Late Cretaceous.

All of the Ulan Suhai ornithomimid material occurs in a single horizon of a siltstone containing thin rhythmites and flaser bedding, which overlies a thick gypsum layer. The ornithomimid horizon is 13 m above the siltstone-gypsum contact. The only conglomeratic sediments found near the locality are 17 m above the ornithomimid horizon. Little postmortem transportation of the ornithomimid skeletons is likely, because all recovered skeletons are intact and fragile skeletal parts (e.g., skull bones and gastralia), as well as large elements (e.g., limbs and vertebrae) are articulated (Figs. 2, 3).

Material and methods

Among fourteen recovered skeletons, there are eleven juveniles and three subadults to adults (Fig. 4). IVPP-V11797-10
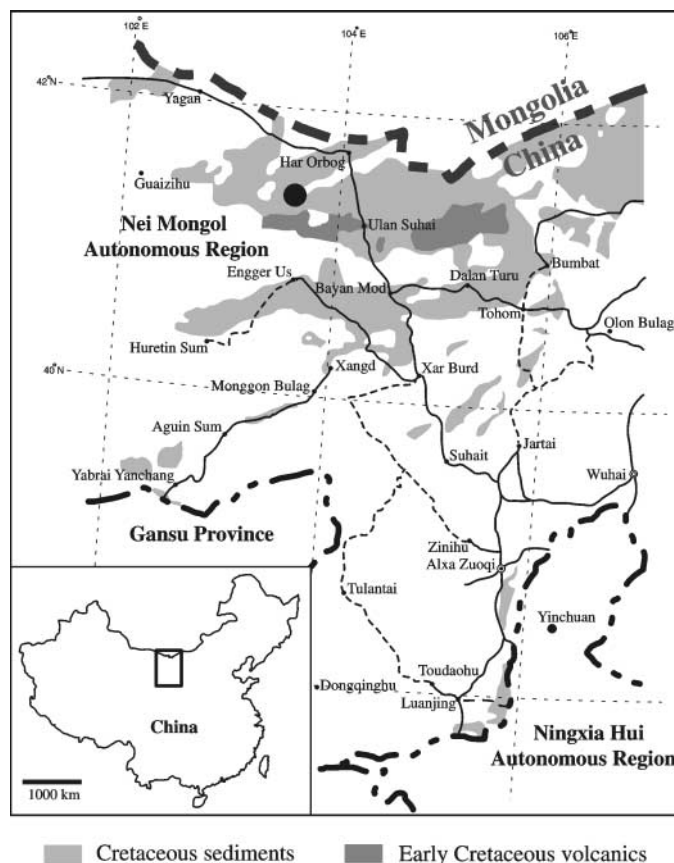

Fig. 1. Map of Nei Mongol (Inner Mongolia) Autonomous Region of China, showing the Ulan Suhai locality (large black dot).

has a 32 cm long left femur and is smaller than IVPP-V11797-19 (24.6 cm long ulna) and IVPP-V1797-29 (femur 41 cm long). The description of the Ulan Suhai ornithomimid is based mainly on IVPP-V11797-10 because it has the best preservation. Additional specimens used for this study include eight complete or nearly complete skeletons (IVPP-V11797-1, IVPP-V11797-2, IVPP-V11797-3, IVPP-V11797-11, IVPP-V11797-12, IVPP-V11797-13, IVPP-V11797-14, and IVPP-V11797-15). Some of the juveniles are articulated but lack most skeletal elements because of erosion. IVPP-V11797-9 is missing the skull and posterior caudal vertebrae. IVPP-V11797-16 preserves the cervical vertebrae, pectoral girdle, forelimbs, and gastroliths. IVPP-V11797-17 is the anterior part of a skull plus cervical vertebrae. Associated material from the locality includes IVPP-V11797-18 (right ulna, radius, metacarpals, and manual phalanges), IVPP-V11797-19 (left ulna), IVPP-V11797-20 (coracoid), IVPP-V11797-21 (sacral vertebrae, ischia, and partial femur), IVPP-V11797-22 (right femur), IVPP-V11797-23 (left hindlimb), IVPP-V11797-24 (left tibia, fibula, and partial femur), IVPP-V11797-25 (proximal end of right femur), IVPP-V11797-26 (left metatarsals, pedal phalanges, and partial astragalus and tibia), IVPP-V11797-27 (caudal vertebra), IVPP-V11797-28 (proximal caudal vertebra), IVPP-V11797-29 (femur, tibia, fibula, metatarsals, and phalanges),
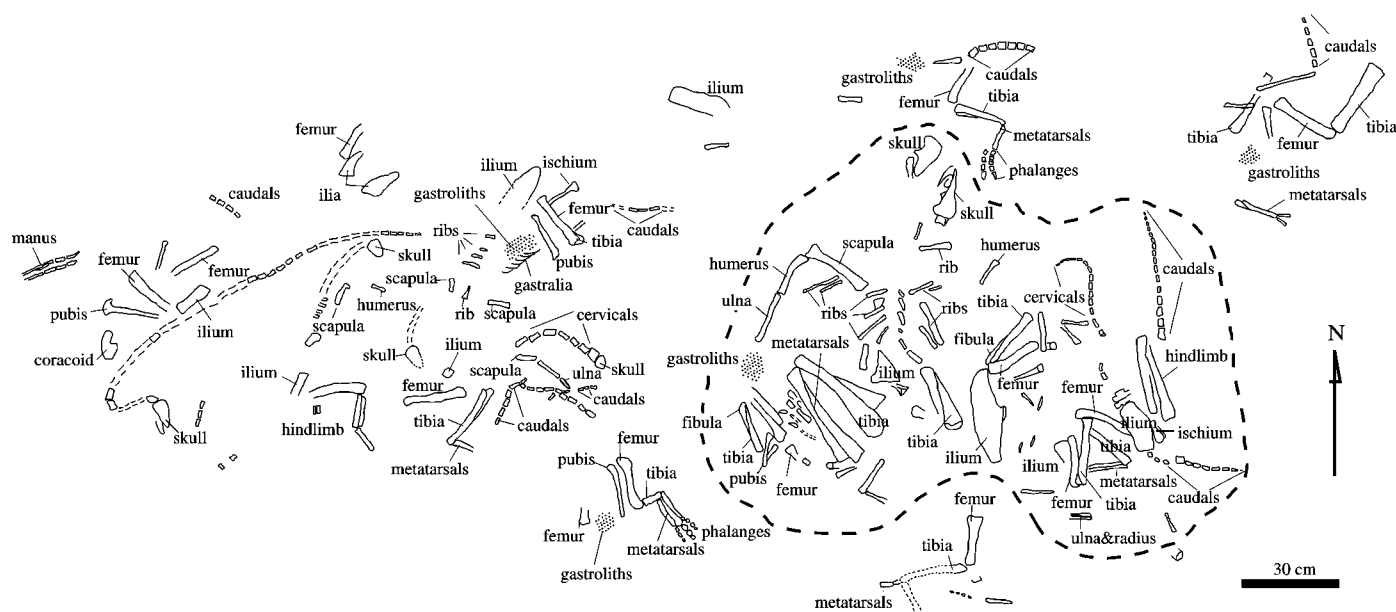
Fig. 2. Bone distribution map at the Ulan Suhai locality. The dotted line shows the approximate area of the large block drawn in Fig. 3.

IVPP-V11797-30 (three caudal vertebrae), IVPP-V11797-31 (occipital region of a skull), IVPP-V11797-32 (caudal vertebra), IVPP-V11797-33 (sacral vertebra), and IVPP-V11797-34 (left ilium and sacral vertebrae).

Padian et al. (1999) used a node-based definition of Ornithomimosauria: *Pelecanimimus* and *Ornithomimus* and all descendants of their most recent common ancestor, which is similar to Ornithomiminae of Sereno (1998). This study follows the definition of Padian et al. (1999) because it is most concordant with the traditional usage of Ornithomimosauria. The "Ornithomimosauria" of Sereno (1998) is different and is a stem-based definition (all maniraptoriforms closer to *Ornithomimus* than Neornithes), consisting of Therizinosauridae, Alvarezsauridae, and Ornithomimidae. Some other taxa (*Deinocheirus* and *Timimus*) were proposed as possible ornithomimosaurs (Barsbold and Osmólska 1990; Rich and Rich 1994). However, their taxonomic positions as ornithomimosaurs are not adequately supported (Makovicky et al. in press). Osteological terminology used in this paper is from Witmer (1997) for cranial pneumatic structures, Nicholls and Russell (1985) for forelimbs, and Makovicky (1995) for the vertebral column. Based on the description of vertebral series in *Ornithomimus* sp. (TMP 95.110.1) by Makovicky (1995), the cervical, dorsal and caudal vertebral series can each be divided into anterior and posterior segments.

Institutional abbreviations.—AMNH, American Museum of Natural History, New York; GIN, Paleontological Center of the Mongolian Academy of Sciences, Ulaanbaatar, Mongolia; IVPP, Institute of Vertebrate Paleontology and Paleoanthropology, Beijing, China; ROM, Royal Ontario Museum, Toronto, Ontario; TMP, Royal Tyrrell Museum of Palaeontology, Drumheller, Alberta; UCMZ, Museum of Zoology, University of Calgary, Calgary, Alberta.

Systematic palaeontology

Dinosauria Owen, 1842
Theropoda Marsh, 1881
Ornithomimosauria Barsbold, 1976
Ornithomimidae Marsh, 1890 *sensu* Smith and Galton 1990
Sinornithomimus gen. nov.

Etymology: Latin *Sinae*, refers to occurrence in China; Greek *ornithos*, bird, and *mimus*, mimic.

Generic diagnosis as for the species.

Sinornithomimus dongi sp. nov.

Etymology: Named after Professor Zhi-Ming Dong, who discovered these skeletons and made great contributions to the Mongol Highland International Dinosaur Project.

Holotype: IVPP-V11797-10; a nearly complete skeleton of a subadult individual with a 32 cm long femur (estimated body length is 2.5 m) but lacks the posterior caudal vertebrae.

Locality and age: Skeletons were discovered from a locality (41˚17'10''N, 103˚52'38''W) near Ulan Suhai in Alashanzuo Banner, Nei Mongol Autonomous Region of China. The locality is in the Ulansuhai Formation and its age is considered to be early Late Cretaceous.

Diagnosis.—An ornithomimid dinosaur with the following apomorphies: depression on dorsolateral surface of posterior process of parietal, fenestra within quadratic fossa divided into two by vertical lamina, low ridge on ventral surface of parasphenoid bulla, and loss of posterolateral extension of the proatlas.

Description.—The holotype skull is transversely crushed. It is intact except for some elements within the orbital region and the mandibular fenestrae that are somewhat displaced
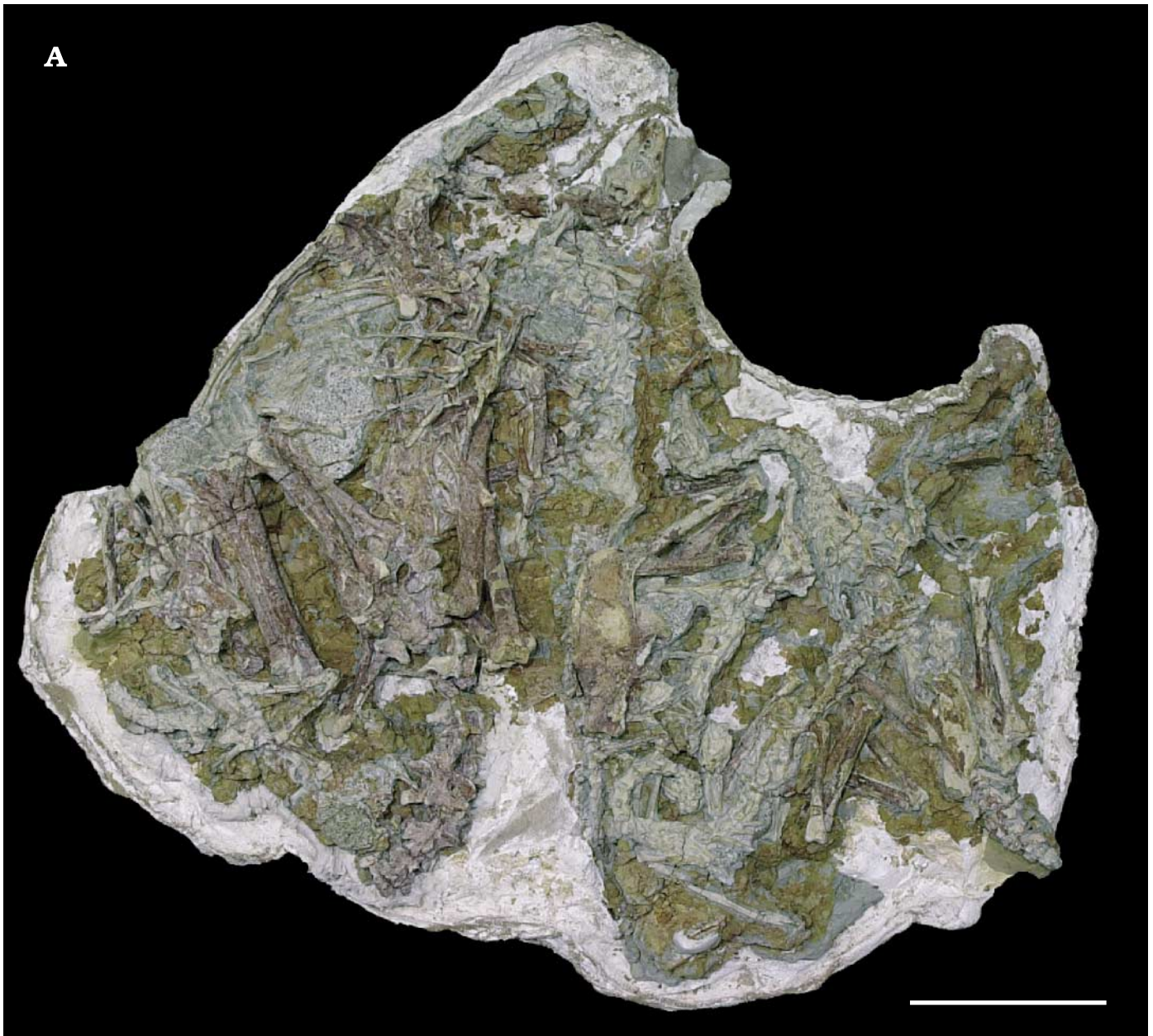
from their original positions (Fig. 5). Some braincase (latero-sphenoid, prootic, and orbitosphenoid) and palatal (vomer and basipterygoid) bones are crushed or not exposed.

Skull length is less than half of the length of the cervical series (Table 1). The orbit is slightly longer than the antorbital fossa. The anterior border of the antorbital fenestra is straight and vertical as in *Garudimimus brevipes* and *Ornithomimus* sp. (TMP 95.110.1). In IVPP-V11797-11 (Fig. 6), the oval (anteroposteriorly long axis) supratemporal fenestra is enclosed by the parietal and squamosal and opened posterodorsally. The supratemporal fossa is large and extends onto the posterior portion of the frontal.

The edentulous premaxilla (Figs. 5, 6) has thin and poste-riorly narrowing nasal and maxillary processes that terminate anterior to the antorbital fossa. The dorsal edge of the

Table 1. Measurements (in mm) of the skull and major body parts in the holotype of *Sinornithomimus dongi* gen. et sp. nov. (IVPP-V11797-10).

| Skull length (premaxilla-squamosal)	183.1
Skull height (including mandible) at the orbit	65.7
Orbit, anteroposterior length of orbit	53.1
Antorbital fossa, length and height	48.5 × 29.4
Antorbital fenestra, anteroposterior length	30.2
Cervical vertebral series, total length	410
Dorsal vertebral series, total length	510
Forelimb, total length	540
Hindlimb, total length	1040
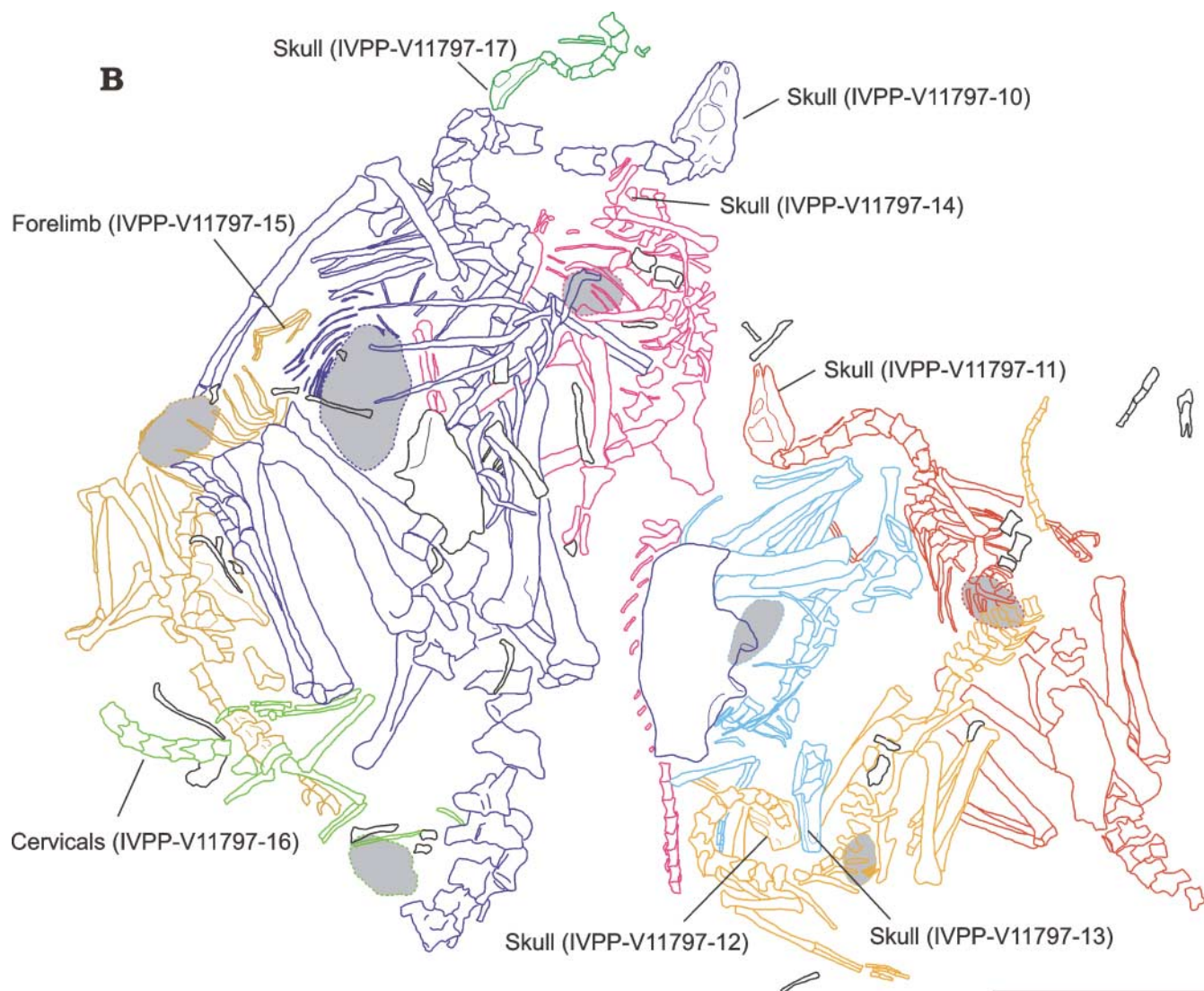
Fig. 3. Largest block, containing eight complete and partial skeletons of *Sinornithomimus dongi* gen. et sp. nov., recovered from the Ulan Suhai locality: photograph (**A**) and explanatory drawing of the same (**B**). Gray areas in B indicate the gastrolith masses. Scale bars 30 cm.

maxillary process contacts the nasal, separating the maxilla from the external narial opening. Anteriorly, the ventral border of the premaxilla curves dorsally, which leaves a gap with the ventrally curved anterior portion of the dentary. In dorsal view, the outer edge of the premaxilla is U-shaped unlike *Struthiomimus* and other North American taxa (Makovicky et al. in press). A series of foramina is present along the ventral edge of the premaxilla. There is a foramen associated with a groove at the base of the internarial plate. The ventral surface of the premaxilla takes part in the palate, and the peripheral margin extends more ventrally than the palate, forming a bony beak.

The maxilla (Figs. 5, 6) has long, thin dorsal and posterior processes. The dorsal process contacts the anterior process of the lacrimal at the midpoint of the antorbital fenestra, and the ventral process thins posteriorly and meets the jugal. There are no foramina posterior to the premaxilla-maxillary suture

along the ventral margin of the maxilla as seen in *Gallimimus bullatus* (GIN 100/1133). The convex ventral margin of the main body of the maxilla expands ventrally as strongly as in *Garudimimus brevipes* and *Gallimimus bullatus*. The expansion meets the dorsomedially directed dorsal margin of the dentary to form a cutting edge. Within the antorbital fossa, there are two accessory (promaxillary and maxillary) fenestrae.

The nasal (Figs. 5, 6) is anteroposteriorly long and transversely narrow. The anterior border of this element is concave where it forms the posterior border of the external narial opening. The nasals contact each other along a straight suture, but the posterior nasals ends diverge lateral to the anterior ends of the frontals and terminate anterior to the prefrontal-lacrimal contact.

In dorsal view, the frontals are triangular (Figs. 5, 7). Each is slightly shorter anteroposteriorly than the nasal, and is the widest close to the posterior edge along the frontal-pa-
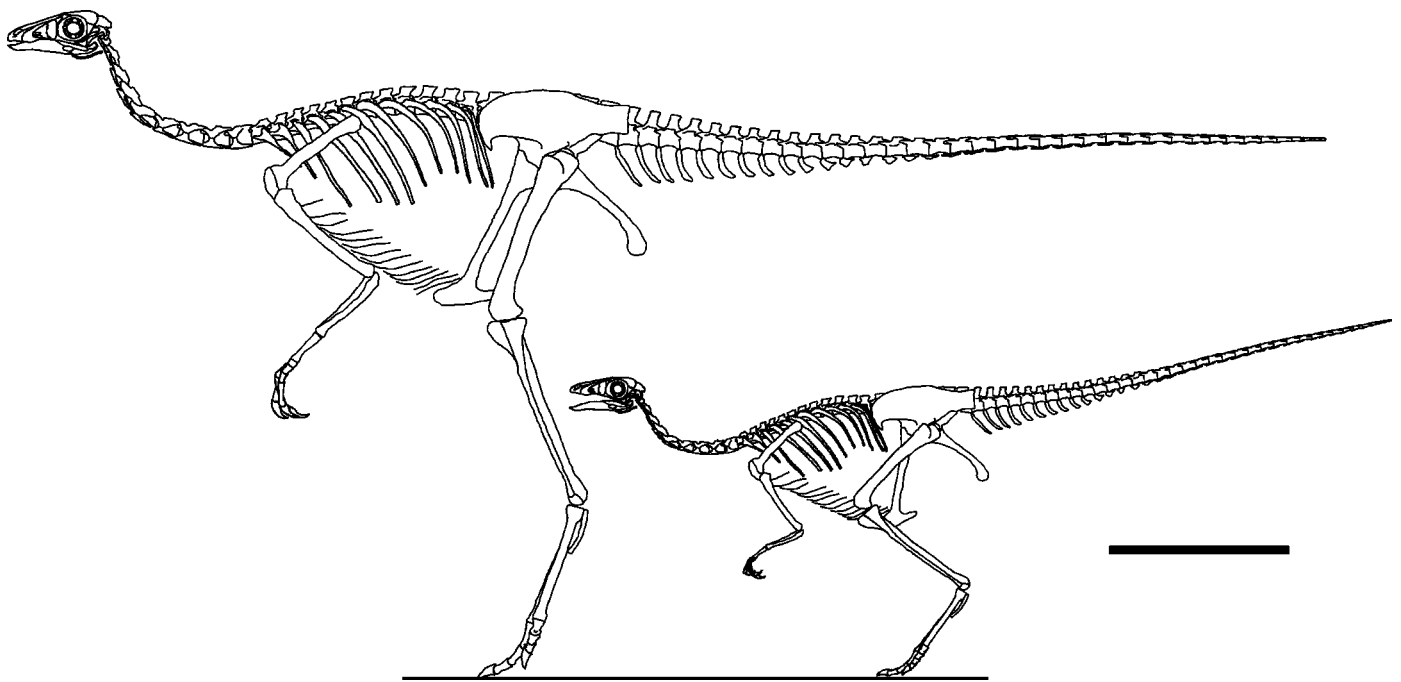
Fig. 4. Reconstructed skeletons of *Sinornithomimus dongi* gen. et sp. nov. (subadult, IVPP-V11797-10; juvenile, IVPP-V11797-11). Scale bar 30 cm.

rietal suture. The posterior quarter (behind the posterior end of the orbit) is inclined ventrally and is domed on each side. The dome of one frontal is separated from the other by a slight depression as in *Gallimimus bullatus* (Osmólska et al. 1972). The lateral slope of the dome forms part of the anterior portion of the supratemporal fossa although the frontal does not participate in the supratemporal fenestra.

The postorbital (Fig. 5) is dorsoventrally elongate with an anteroposteriorly expanded dorsal end. The posterior side (anterior border of the infratemporal fenestra) of the element is concave dorsally and convex ventrally. Ventrally, it narrows along the medial side of the jugal. The posterodorsal process contacts the lateral side of the anterior process of the squamosal.

Medially the parietals (Fig. 7) are horizontally flat, forming the posterior part of the skull table. A posterolateral process extends beyond the posterior end of the skull table. The dorsolateral surface of the process has a depression unlike *Struthiomimus* sp. (TMP 90.26.1), and the distal tip fits onto the top of the paroccipital process. The lateral side of the skull table and the lateral surface of the posterior process form the concave margin of the supratemporal fossa.

The main body of the squamosal (Figs. 6, 7) has medial, anterior, ventral, and posterior processes. The medial process contacts the parietal and forms the posterior boundary of the supratemporal fenestra. The long anterior process fits onto the medial side of the posterodorsal process of the postorbital. The ventral process, exposed laterally, is as long as the anterodorsal process and terminates between the quadrate and quadratojugal (Fig. 7A, E). The posterior process is short, and its ventral border is concave for articulation with the quadrate. At the base of the posterior process, the lateral surface of the

left squamosal in IVPP-V11797-31 preserves the squamosal recess as in *Dromiceiomimus brevitertius* Parks, 1926 and tyrannosaurids (Witmer 1997).

The lacrimal is almost L-shaped with long anterior and ventral processes and a short posterior process (Figs. 5, 6). The posterior part of the lacrimal overlies and fits into a depression in the prefrontal. The prefrontal is nearly equal to the lacrimal in size in dorsal view and has posterior and ventral processes of sub-equal length. The anterior end contacts the nasal, separating the lacrimal from the frontal. The posterior process of the prefrontal plugs into a depression on the ventrolateral surface of the anterior portion of the frontal. The ventral process narrows and is sutured onto the medial side of the ventral process of the lacrimal.

The jugal is anteroposteriorly long with an expanded posterior end (Figs. 5, 6). The anterior end is not bifurcated for its contacts with the maxilla and lacrimal in contrast to *Struthiomimus* sp. (TMP 90.26.1) and *Ornithomimus* sp. (TMP 95.110.1). The expanded posterior end has an anteroposteriorly elongate depression for the quadratojugal. A long process near the posterior end of the jugal extends posterodorsally and meets the posterior side of the postorbital. The posterior border of the process forms the concave ventral border of the infratemporal fenestra.

The quadratojugal, well preserved in IVPP-V11797-31, is L-shaped with dorsal and anterior processes (Fig. 7). The dorsal process is much longer than the anterior process and contacts the ventral process of the squamosal anteriorly. The process does not bifurcate at the dorsal end, and the ventral half of the process forms the weakly concave anterior border of the paraquadratic foramen, but lacks a distinct notch such
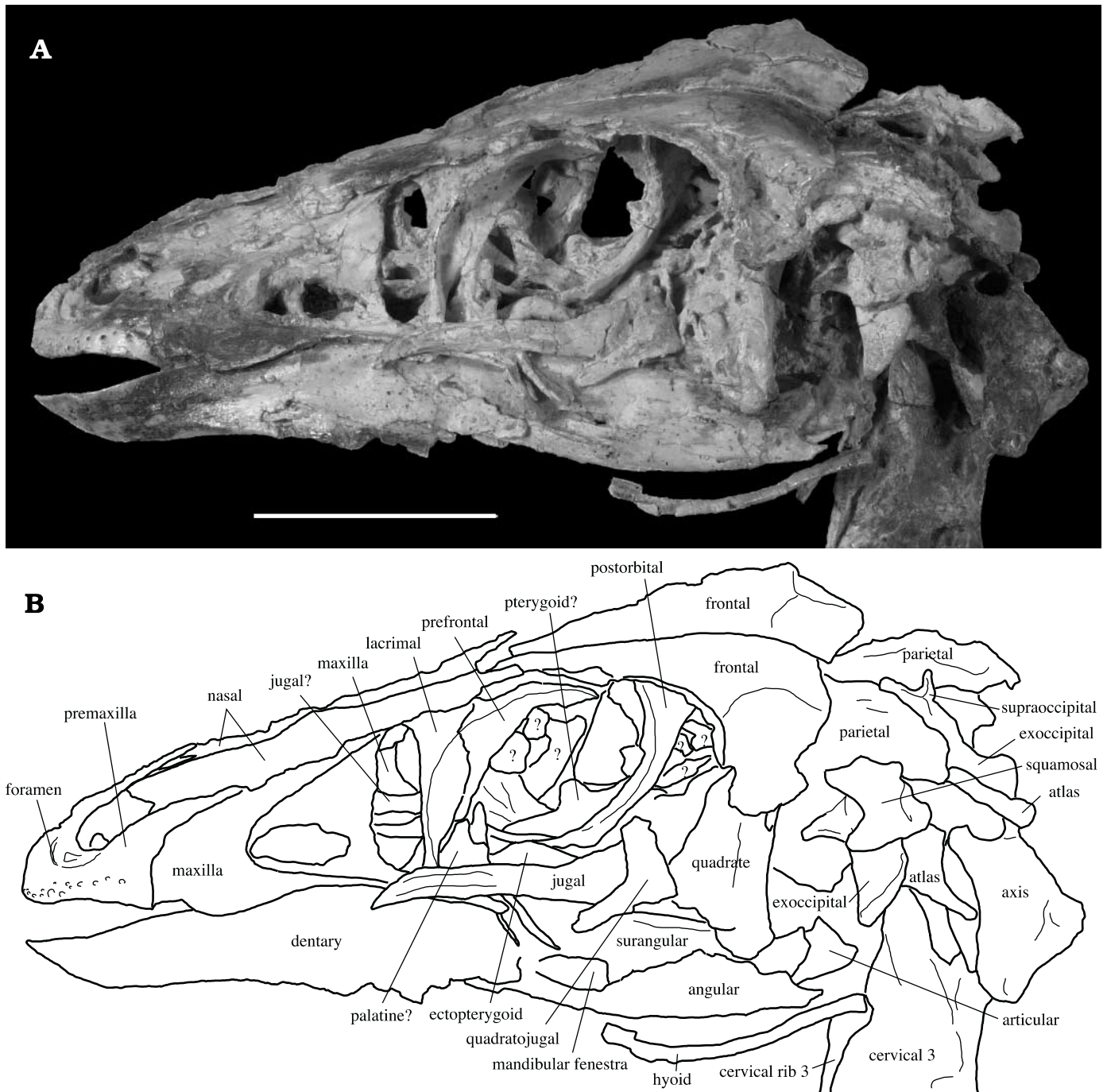
Fig. 5. Skull of *Sinornithomimus dongi* gen. et sp. nov. (IVPP-V11797-10) in left lateral view. Photograph (**A**) and explanatory drawing of the same (**B**). Scale bar 5 cm.

as found in *Ornithomimus* sp. (TMP 95.110.1) (Makovicky et al. in press). The posteroventral part of the element forms a square corner, and is sutured to the lateral side of the accessory condyle of the quadrate.

The mandibular condyles of the quadrate (Figs. 5–7) are roughly equal in size and are well separated by an anteroposterior sulcus. Lateral to the lateral condyle there is an accessory condyle. The accessory condyle is more dorsally positioned than the mandibular condyles and is contoured to the dorsally expanded region of the surangular. In posterior view,

there is a slight concavity for the paraquadratic foramen. This concavity is dorsal to the accessory condyle (Fig. 7D, H). On the mid-posterior surface of the main body, an oval-shaped fossa is present as in other ornithomimosaurs (Makovicky and Norell 1998). A fenestra found within the quadratic fossa, is roughly half of the fossa in size, and is divided by a vertical lamina (Fig. 7D, H). The quadrate has a large pterygoid wing. Its anteroposterior length is roughly 40% of the quadrate height. The ventral portion of the pterygoid wing forms a medially extending shelf, where it contacts the pterygoid.
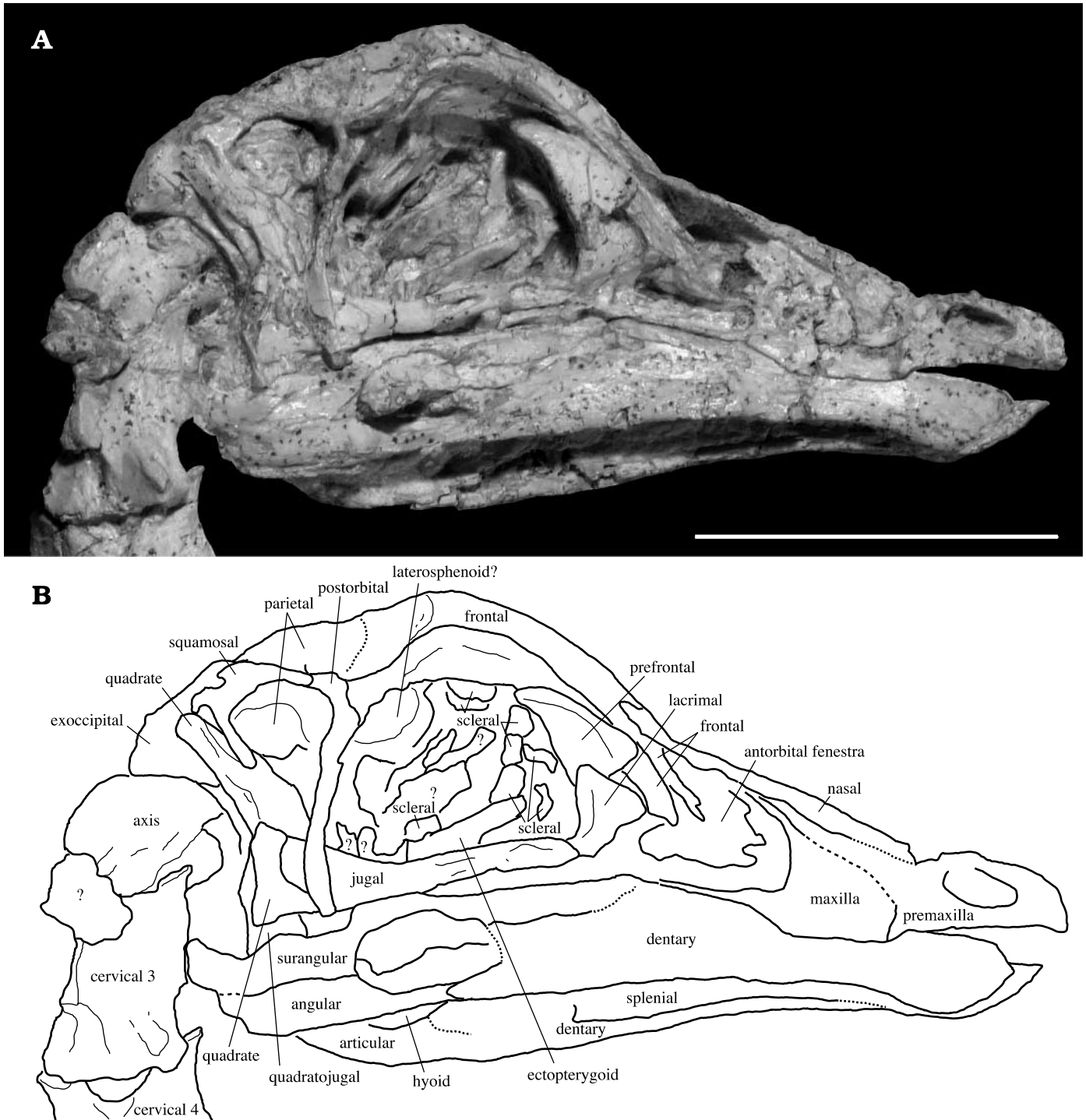
Fig. 6. Juvenile skull of *Sinornithomimus dongi* gen. et sp. nov. (IVPP-V11797-11) in right lateral view. Photograph (**A**) and explanatory drawing of the same (**B**). Scale bar 5 cm.

Dorsally, the supraoccipital is flat and lies between the posterior processes of the parietals (Figs. 5, 7). The posterior surface has a vertical ridge as in *Struthiomimus altus* (Lambe, 1902) (AMNH 5355), but unlike *Gallimimus bullatus* (Makovicky and Norell 1998). In dorsal view, the dorsal process is thin and U-shaped.

The paroccipital process (Figs. 5, 7) extends latero-ventrally, and its ventral border is lower than the foramen magnum. The exoccipital is pneumatic with a large foramen at mid-length, whereas basally it is penetrated on the anterior side as seen in *Gallimimus bullatus* (GIN 100/987) (fig. 1F in Makovicky and Norell 1998). The foramen at the mid-length is also seen on the posterior surface of the paroccipital process in *Gallimimus bullatus* (GIN 100/1133) and *Struthiomimus* sp. (TMP 90.26.1). A posteroventral process, extending from the base of the paroccipital process, borders the lat-
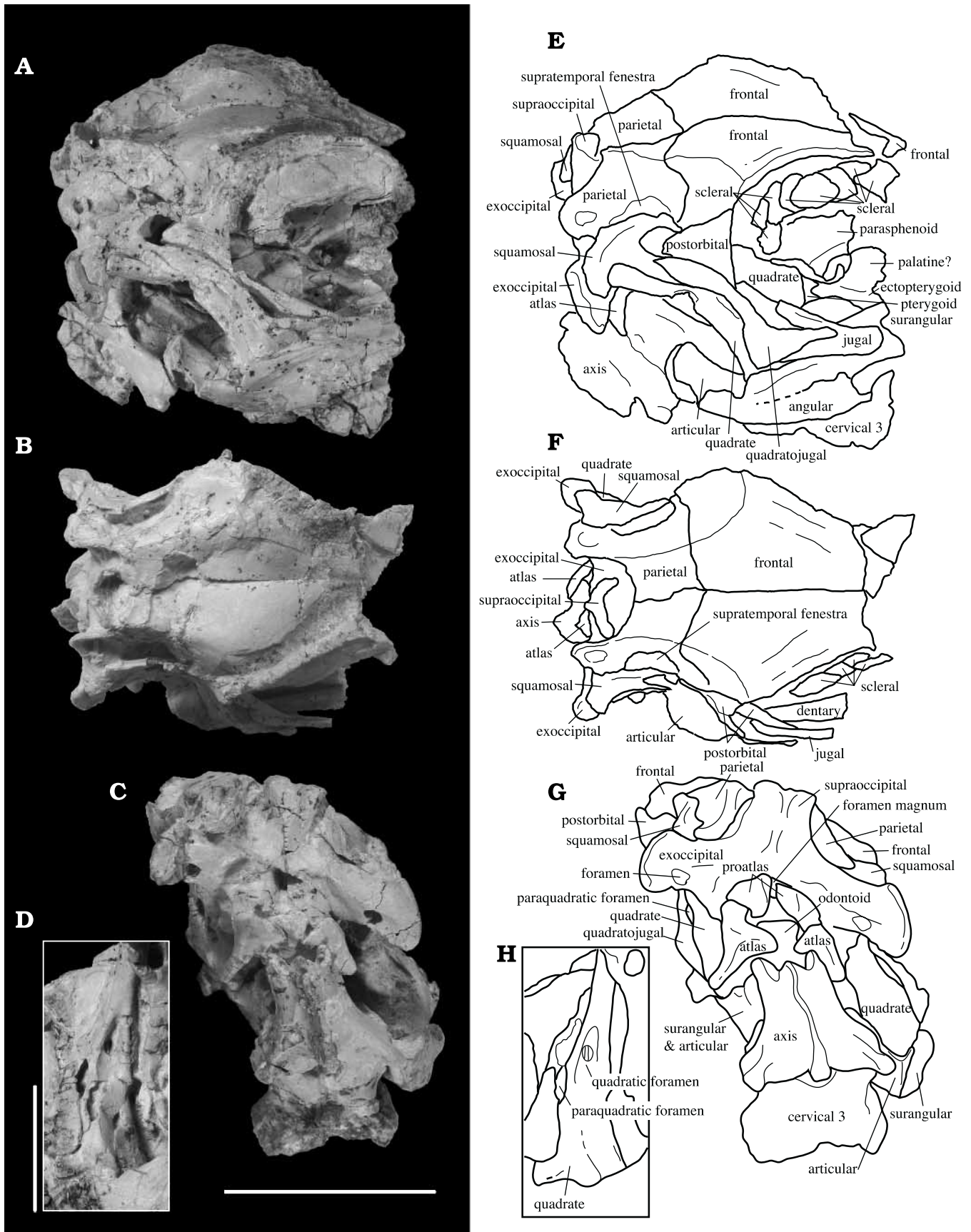
Fig. 7. Juvenile skull of *Sinornithomimus dongi* gen. et sp. nov. (IVPP-V11797-31) in lateral (**A**, **E**), dorsal (**B**, **F**), occipital (**C**, **G**), and posterolateral views, showing the structure of the quadrate region (**D**, **H**). Scale bar below C represents 3 cm and is for A–C and E–G. Scale bar left of D is 2 cm.
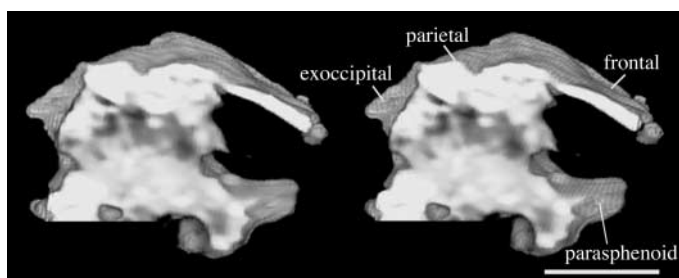
Fig. 8. Stereographs (CT images) of the bulbous parasphenoid of *Sinornithomimus dongi* gen. et sp. nov. (IVPP-V11797-31). Scale bar 3 cm.

eral side of the foramen magnum. Its ventral end forms a dorsal portion of the occipital condyle. The metotic strut extends ventrally from the base of the paroccipital process. Its lateral surface is smooth. Ventrolateral to the occipital condyle and medial to the metotic strut, a depression is associated with foramina for the vagus (X) and hypoglossal (XII) nerves. The foramen for the vagus nerve (X) is more laterally positioned and slightly larger than the ones for nerve XII. Pneumatic structures anterior to the metotic strut in IVPP-V11797-10 are not visible because of crushing.

The parasphenoid is partially exposed in IVPP-V11797-31 (Figs. 7, 8). It has the bulbous structure typical of ornithomimosaurs and troodontids. It is wide posteriorly and has an anterior process (parasphenoid rostrum) as in *Gallimimus bullatus* (Osmólska et al. 1972). The bulbous portion has a flat ventral surface. The parasphenoid rostrum is roughly half of the height of the bulbous portion of the element in lateral view, and it becomes narrower anteriorly in ventral view. In lateral view, the process has a horizontal dorsal edge at the same level as the dorsal border of the bulbous portion. Dorsoventrally, it narrows dramatically as the ventral border curves anterodorsally, whereas the anterior process narrows gradually in *Garudimimus brevipes* and *Gallimimus bullatus* as well as in the troodontids *Saurornithoides* and *Troodon* (Osmólska et al. 1972; Barsbold 1981; Currie 1985). The base of the anterior process has a low ridge unlike *Gallimimus bullatus*.

The posterior portion of the pterygoid is preserved in IVPP-V11797-31. Posteriorly the pterygoid contacts the medial surface of the pterygoid wing of the quadrate. At the base of the quadrate wing, a short basipterygoid process extends posteromedially. In IVPP-V11797-10, although the main body of the ectopterygoid is crushed, the hook-shaped jugal process of the element is exposed. The distal end of the process reaches the middle of the jugal.

The anterior portions of the dentaries curve ventrally (Figs. 5, 6). The symphyseal region of the paired dentaries is U-shaped in ventral view. The radius of the dorsal margin of the arc is less than that of the ventral margin of the joined premaxillae. The lateral side of the dentary, below the ventral expansion of the maxilla, has a foramen as in *Gallimimus bullatus* (Hurum 2001) but lacks the series of foramina that are found in *Pelecanimimus polyodon* Perez-Moreno, Sanz, Buscalloni, Meratalla, Ortega, and Rasskin-Gutman, 1994, *Ornithomimus* sp. (TMP 95.110.1), *Struthiomimus* sp. (TMP

90.26.1), and *Gallimimus* sp. (GIN 950818). The dorsal edge of the dentary is sharp in the anterior two-thirds of the element and more rounded in the posterior third. A ventral process at the posterior end laterally overlaps the anterior process of the angular. The splenial and prearticular are not exposed.

The dorsal border of the surangular is convex in lateral view and has an anteroposteriorly oriented ridge anterior to the retroarticular process for an articulation with the accessory condyle of the quadrate (Figs. 5, 7). The posterior surangular foramen is absent. The suture with the angular originates at the posterior end of the mandibular fenestra and extends to the posterior end of the retroarticular process as in *Ornithomimus* sp. (TMP 95.110.1) and *Struthiomimus* sp. (TMP 90.26.1). The lateral surface of the long anterior process of the angular has a shallow groove for the surangular contact. The articular is not well exposed.

The posterior part of a thin and long hyoid (Fig. 5) is preserved ventral to the angular in a similar position to that described in *Pelecanimimus polyodon* (Pérez-Moreno et al. 1994). It is slightly curved in lateral view, following the outline of the ventral edge of the lower jaw, and expands slightly at its posterior end. The anterior portion of the hyoid is preserved in IVPP-V11797-31. It is thicker than in IVPP-V11797-10 and curves medially and anteriorly.

Postcranial skeleton

The cervical and dorsal vertebrae are articulated in the holotype, but the sacral and caudal vertebrae are displaced from their original positions. The neurocentral sutures in the holotype are fused in all of the cervical and the anterior three dorsal vertebrae. Those of the rest of vertebrae are unfused, which may indicate that the closure of the neurocentral sutures proceeds from the cervical vertebrae posteriorly.

The paired proatlas is preserved in IVPP-V11797-31 (Fig. 7C, G). Each element is triangular in shape and lacks any posterolateral extension. The atlas neural arches are preserved in IVPP-V11797-10 and IVPP-V11797-31, but the atlantal intercentra are not exposed (Figs. 7C, G, 9). The neural arch is separated into two neurapophyses, which are roughly equal in size. In *Gallimimus bullatus* (Osmólska et al. 1972), the right half is larger than the left one, which may be a peculiarity of the individual. The postzygapophyses gradually thin posteriorly, whereas the postzygapophyses in *Gallimimus bullatus* are constant in thickness and have rounded posterior ends (Osmólska et al. 1972). The pedicels are shorter than the posterior processes as in *Gallimimus bullatus*.

The axis (exposed in IVPP-V11797-10, IVPP-V11797-11, and IVPP-V11797-31) has a rounded neural spine in lateral view (Figs. 5–7, 9). In dorsal view, the neural arch flares posteriorly with small prezygapophyses and large postzygapophyses. It has a straight posterior border. The horizontal articular surface of the postzygapophysis is circular in ventral view. The epiphysis extends slightly more posteriorly
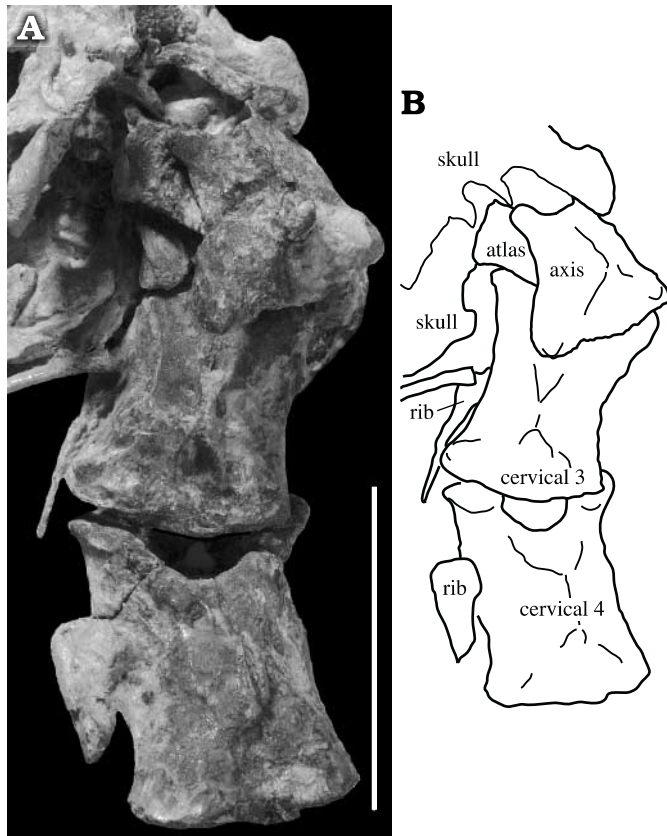
fifth and sixth cervicals (third and fourth in *Ornithomimus* sp. (TMP 95.110.1)).

The posterior cervical vertebrae (sixth to tenth) are distinguished from the anterior cervical series in having long postzygapophyses (Fig. 11). The neural spines are not well preserved, but their positions shift more anteriorly on the neural arch primarily because of the shortening of the prezygapophyses and the elongation of the postzygapophyses. The bases of the postzygapophyses extend posterolaterally, but the posterior halves of the postzygapophyses are directed more laterally as in *Gallimimus bullatus* and *Ornithomimus* sp. (TMP 95.110.1) but unlike *Harpymimus okladnikovi* Barsbold and Perle, 1984 (where they are almost parallel). The infradiapophyseal fossae are larger than the infrapostzygapophyseal fossae in the eighth and ninth cervicals. The lateral side of the eighth cervical vertebra has a central pneumatic fossa (10 mm long and 6 mm high) just dorsal to the parapophysis. The ventral surfaces in the eighth to tenth cervical centra preserve pairs of well-developed parapophyses at the anterior ends. The centra of posterior cervical vertebrae are taller than the anterior cervical vertebrae.

Eleven dorsal vertebrae are exposed in the holotype (Fig. 12). The neural arches of the first to fifth dorsal vertebrae are
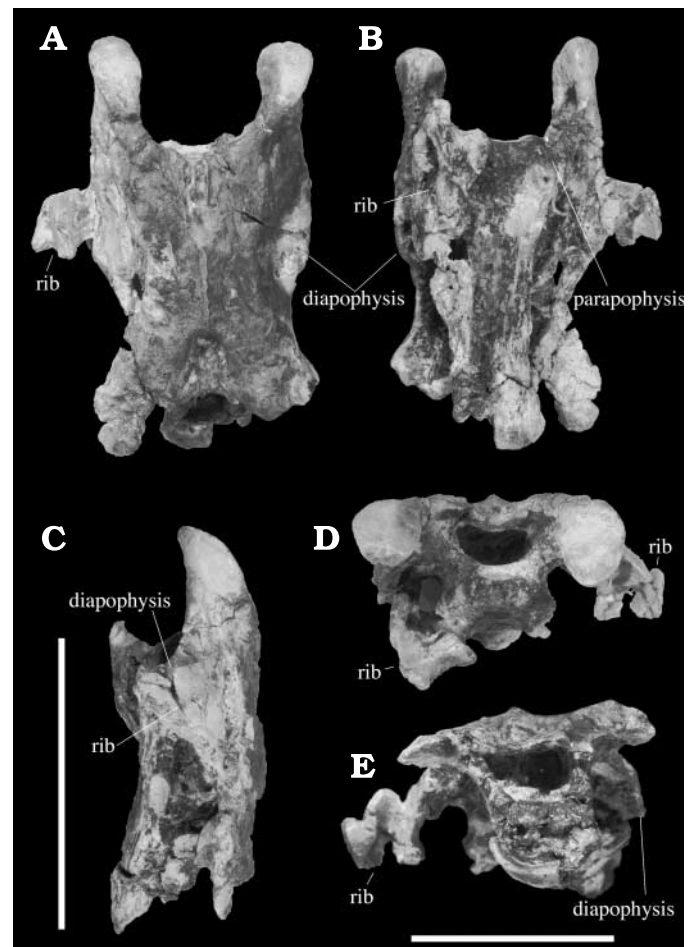

Fig. 9. Anterior cervical vertebrae of *Sinornithomimus dongi* gen. et sp. nov. atlas, axis and the third and fourth cervical vertebrae in IVPP-V11797-10 in dorsal view; photograph (**A**) and explanatory drawing of the same (**B**). Scale bar 3 cm.

than the posterior end of the postzygapophysis and is as strong as those of *Gallimimus bullatus* and *Ornithomimus* sp. (TMP 95.110.1).

Anterior cervical vertebrae (from the third to fifth) have long prezygapophyses (Figs. 5, 6, 9, 10). The anteroposterior length of each neural arch is much longer than that of the axis, and they become even longer posteriorly (Table 2). The neural spines are positioned posterior to the mid-lengths of the neural arch unlike *Gallimimus bullatus* and *Ornithomimus* sp. (TMP 95.110.1) (Osmólska et al. 1972; Makovicky 1995). The spines are low, and anteroposterior lengths range from one-fourth to one-fifth of the neural arch height as in *Ornithomimus* sp. (TMP 95.110.1) (Makovicky 1995). In dorsal view, the posterior border of the neural arch is straight transversely in the third and fourth cervicals because the postzygapophyses are connected by a lamina. The postzygapophyses in the fifth are longer and are separated. The concave posterior intervertebral articular surfaces of the third and fourth cervicals are exposed and are nearly perpendicular to the main axes of the centra in lateral view. The anterior intervertebral articular surface of the fifth cervical is nearly vertical but the posterior surface of the fifth (Fig. 10) and anterior surface of the sixth are strongly inclined anterodorsally and anteroventrally respectively, indicating that the strongest curvature of the neck of *Sinornithomimus dongi* occurs in the

Fig. 10. Fifth cervical vertebra of *Sinornithomimus dongi* gen. et sp. nov. (IVPP-V11797-10) in dorsal (**A**), ventral (**B**), lateral (**C**), anterior (**D**), and posterior (**E**) views. Scale bars 3 cm.
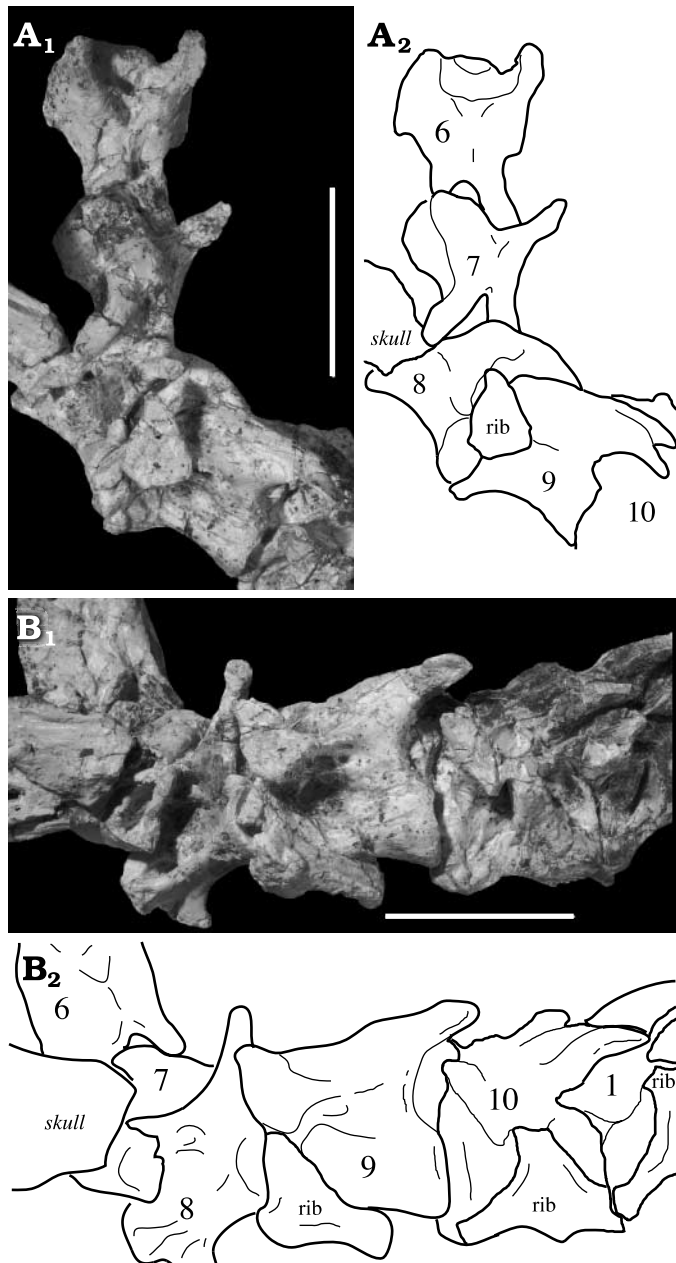
Fig. 11. Posterior cervical vertebrae of *Sinornithomimus dongi* gen. et sp. nov. (IVPP-V11797-10). **A**. Sixth to ninth cervical vertebrae: sixth and seventh in dorsal view and eighth and ninth in lateral view. **B**. Sixth to tenth cervical vertebrae: sixth in dorsal view and eighth to tenth in lateral view. Italicized letters indicate an element from IVPP-V11797-17. Scale bars 3 cm.

Table 2. Lengths (in mm) of cervical, dorsal, and caudal vertebrae in the holotype (IVPP-V11797-10) and sacral centra in a juvenile individual (IVPP-V11797-15) of *Sinornithomimus dongi* gen. et sp. nov. Abbreviations: NAL, neural arch length; CL, centrum length.

Holotype IVPP-V11797-10		NAL	CL
Atlas		23.9	–
Axis		33.5	26.2
Cervicals	#3	50.7	–
	#4	56.1	–
	#5	67.0	52.8
	#6	65.9	–
	#7	64.3	–
	#8	–	47.5
	#9	59.8	46.4
	#10	56.8	43.3
Dorsals	#1	49.2	–
	#2	46.2	–
	#3	45.8	–
	#4	47.5	–
	#5	–	37.6
	#6	–	37.2
	#7	–	39.9
	#8	–	38.7
	#9	–	43.0
	#10	–	44.7
Caudals	#1	–	49.0
	#3	48.7	43.6
	#4	50.1	–
	#5	49.0	44.1
IVPP-V11797-15		NAL	CL
Sacrals	#1	–	28.3
	#2	–	30.9
	#3	–	27.2
	#4	–	26.9
	#5	–	27.5

preserved, but those of the more posterior dorsal vertebrae are missing in the holotype. The neural spines become higher dorsoventrally in more posterior dorsal vertebrae. The prezygapophyses are as short as in the posterior cervicals, but the postzygapophyses are reduced in length from the first to second dorsal vertebrae (30.8 and 17.3 mm respectively). The left parapophysis, exposed on the fourth centrum, is positioned ventral to the neurocentral suture and is circular, approximately 8 mm in diameter. The infraprezygapophyseal, infradiapophyseal, and infrapostzygapophyseal fossae are evenly divided by laminae, but the infraprediapophyseal lamina is weaker than the infrapostdiapophyseal lamina. The infraprediapophyseal lamina becomes weaker in more posterior dorsal vertebrae. Centrum length becomes progressively larger in more posterior dorsal vertebrae (Table 2). The lateral central surface lacks pneumatic features. The ventral surfaces of all exposed dorsal vertebrae lack the hypapophysis and tubercles at the anterior and posterior ends in contrast to *Ornithomimus* sp. (Makovicky 1995).

Six sacral centra in IVPP-V11797-15 (juvenile) are better exposed (Fig. 13) and preserved than in the holotype. The first sacral centrum is similar to the last dorsal centrum and its anterior intervertebral articular surface is positioned slightly anterior to the ventral hook of the ilium. The second and third sacral centra are not well exposed. The ventral surface of the fourth centrum has a shallow sulcus as in *Ornithomimus* sp. (Makovicky 1995). The fourth and fifth centra have parapophyses at the anterior ends of their lateral surfaces. The fourth centrum is wider than high. The fifth centrum is dorsoventrally flattened anteriorly, but is circular in cross-section posteriorly. The posterior part of the lateral
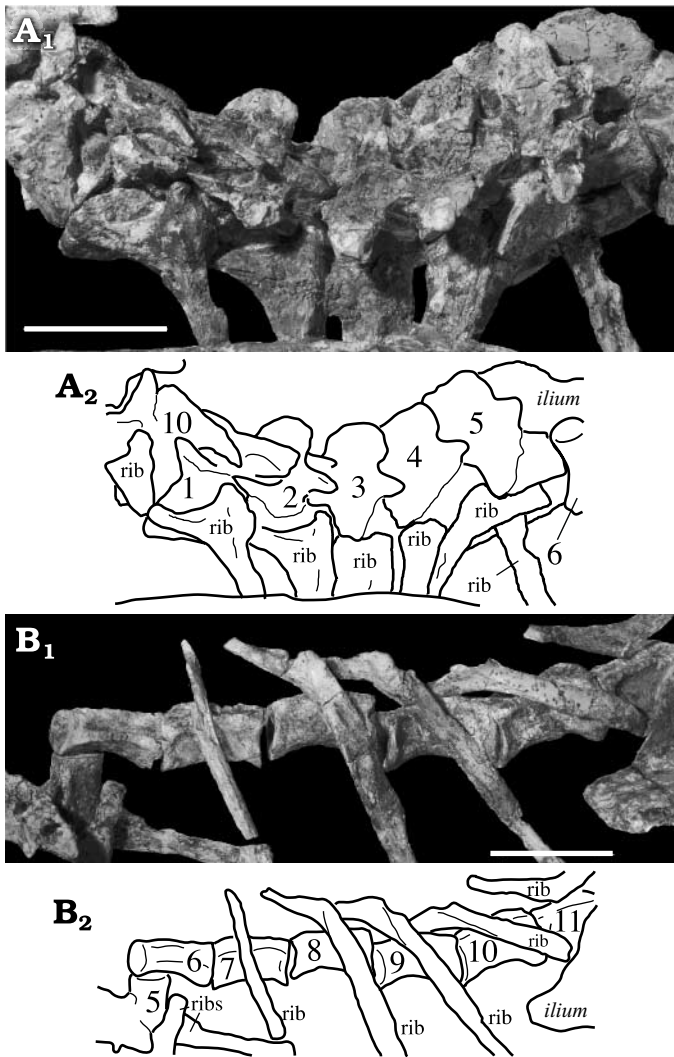
IVPP-V11797-12, -14, and -30 (Fig. 14B) and are characterized by the lack of transverse processes, low neural spines, and long prezygapophyses as in other ornithomimosaurs (Makovicky 1995). The prezygapophyses extend further anteriorly than the anterior intervertebral articular surfaces, and extend approximately 47% of the preceding centrum's length. The centra of the posterior caudal series are low and have sulci on their ventral surfaces.

The proximal end of the last cervical rib is preserved in the holotype (Fig. 11C, D) and its capitulum and tuberculum are subequal in length. Nine left and eight right dorsal ribs are preserved (Fig. 12). The first dorsal rib is short (105 mm long). The second to eighth dorsal ribs (at least) are nearly equal in length (about 200 mm) and have squared-off distal ends, which may be for articulation with the cartilaginous sternum or sternal ribs. The proximal half of each dorsal rib has an anteroposterior, laterally flat extension as in other ornithomimosaurs, although it is less developed than in *Struthiomimus altus*. There are at least fourteen rows of gastralia in IVPP-V11797-9 and each gastralium is segmented into two parts on each side as in *Struthiomimus altus* (Nicholls and Russell 1981). The chevrons of the anterior caudal vertebrae are anteroposteriorly narrow and dorsoventrally long. Posterior chevrons are short dorsoventrally and elongate anteroposteriorly.

As reported by Kobayashi et al. (1999), gastrolith masses are enclosed within the articulated ribcages of all recovered skeletons and are positioned anterodorsal to the pubic boots (Figs. 3, 25). The sizes of the masses are greater in larger individuals (175 X 116 mm in IVPP-V11797-10 and 97 X 75 mm in IVPP-V11797-15). The largest exposed pebbles are

Fig. 12. Dorsal vertebrae of *Sinornithomimus dongi* gen. et sp. nov. (IVPP-V11797-10). **A**. Tenth cervical, and first to fifth dorsal vertebrae. **B**. Fifth to eleventh dorsal centra. Italicized letters indicate elements from IVPP-V11797-14. Scale bars 3 cm.

surface of the fifth centrum has an anteroposteriorly-elongated depression.

Caudal vertebrae in the holotype are disarticulated, and only seven proximal caudal vertebrae are preserved (Fig. 14A). The neural spines of these caudal vertebrae are tall with horizontal dorsal borders, but they become lower in more posterior caudals. The transverse processes are longer than neural spine heights, and the posterior angles between the transverse processes are wider than 120 degrees in dorsal view. The prezygapophyses and postzygapophyses are as short as those of the dorsal vertebrae. The centra are taller than wide, and the anterior and posterior articular surfaces are vertical in lateral view. The lateral surfaces of the centra lack pneumatic features. The ventral surfaces have pairs of tubercles at the anterior and posterior ends (which are more pronounced posteriorly) for articulation with chevrons. Posterior caudal series are preserved in other skeletons such as
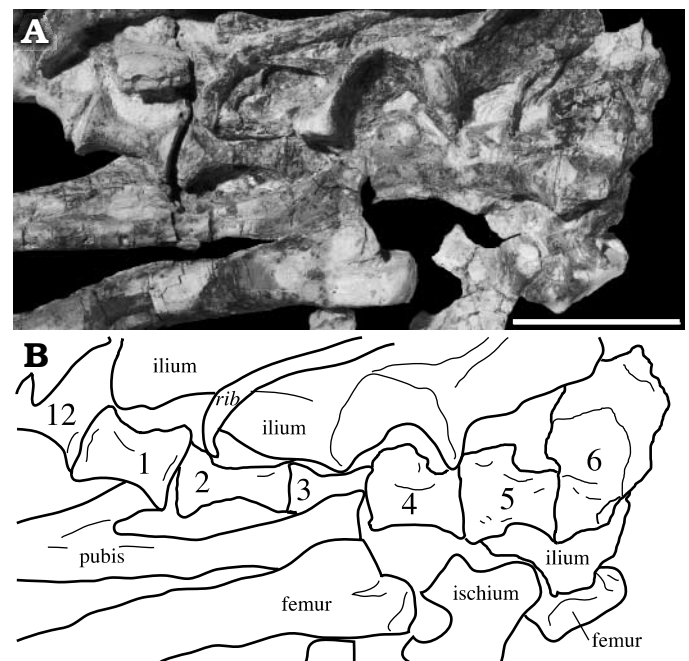

Fig. 13. Sacral vertebrae of *Sinornithomimus dongi* gen. et sp. nov. (IVPP-V11797-15) in ventral view. Italicized letters indicate an isolated element not from IVPP-V11797-15. Scale bar 3 cm.
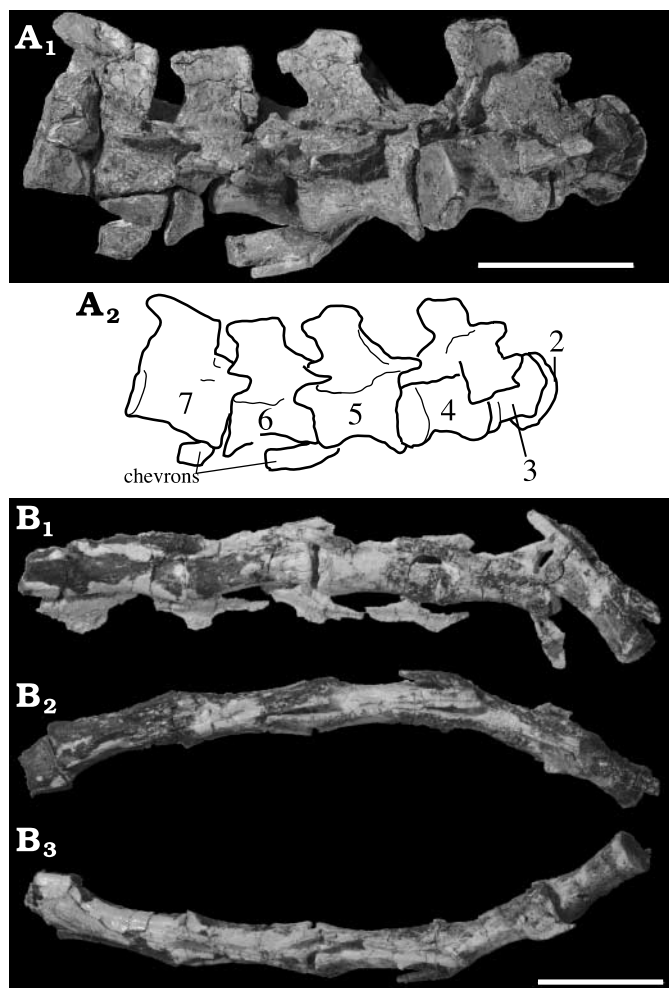
Fig. 14. **A**. Caudal vertebrae of *Sinornithomimus dongi* gen. et sp. nov.: anterior caudal vertebrae of IVPP-V11797-10 in lateral view. **B**. Posterior caudal vertebrae of IVPP-V11797-30 in lateral (B₁), dorsal (B₂), and ventral (B₃) views. The numbers in A₂ indicate the positions of caudal vertebrae. Scale bars 3 cm.

larger in the larger individuals (9 mm in IVPP-V11797-10 and 5.5 mm IVPP-V11797-15).

The scapula (Fig. 15A) is thin and long, and is slightly shorter than the humerus (Table 3). The length ratio of scapula/humerus in *Sinornithomimus dongi* is greater (96%) than in *Gallimimus bullatus* (85%) (Osmólska et al. 1972). The scapular blade expands distally. The acromion process is relatively weak compared with those of *Gallimimus bullatus* and *Struthiomimus altus* (Nicholls and Russell, 1985). A depression is present on the dorsal surface of the supraglenoid buttress in the IVPP-V11797-10 as in *Struthiomimus altus*, *Gallimimus bullatus*, and *Harpymimus okladnikovi*, although it is absent in IVPP-V11797-9. The supraglenoid buttress is associated with a ridge on the lateral surface of the scapula. The ridge is nearly parallel to the scapula-coracoid suture and extends to one-third of the scapular width. The glenoid, formed by the supraglenoid and infraglenoid butresses, faces posterolaterally.

The coracoid (Fig. 15B) is slightly less than half of the scapular length (Table 3). In IVPP-11979-20, its antero-posterior length (103.58 mm) is roughly twice as long as the dorsoventral height (55.28 mm), whereas in *Struthiomimus altus* the coracoid is three times as long as high (Nicholls and Russell 1985). The infraglenoid buttress is aligned with the posterior coracoid process in dorsal view (Fig. 15B). The anterior end of the dorsal surface of the posterior coracoid process lacks a pit, unlike *Dromiceiomimus samueli* (Parks, 1926) (ROM 840) and *Struthiomimus altus* (UCMZ(VP)1980.1). The prominent biceps tubercle is positioned close to the base of the posterior coracoid process (Fig. 15B). The lateral surface has two areas for muscle attachments (M. scapulocoracoideus and M. coracobrachialis longus; Nicholls and Russell 1985), bordered by a weak ridge extending from the biceps tubercle to the anteroventral edge of the element. The coracoid foramen is anterior to the biceps tubercle close to the scapulocoracoid suture.

The humerus (Fig. 16A) is slender. The ratio of width of the proximal end to total length is 0.19. Its shaft is straight in lateral view and slightly laterally curved in dorsal view. The long axis of the distal end of the right humerus is twisted clockwise with respect to that of the proximal end by approximately 20 degrees. The head is strong and is spherical. In dorsal view, the anterior tuberosity is at the same level as the head but the posterior tuberosity is more distally positioned. The deltopectoral crest is relatively weaker than that of *Anserimimus planinychus*, and is most pronounced at one-fifth of its length from the proximal end (at 40.7 mm). The ulnar condyle is larger than the radial condyle. Lateral to the ulnar condyle there is an entepicondyle that is weak in comparison with those of *Anserimimus planinychus* and *Gallimimus* sp. (GIN 950818). The dorsal surface of the distal end is shallowly depressed for the olecranon process of the ulna.

The holotype's ulna and radius are articulated with the humerus (Fig. 16A). The radius is positioned proximally on the ventral side of the ulna but on the medial side distally. The ulna is roughly three-quarters of humerus length (Table 3). The ulna is weakly curved towards the radius. The distal ulna is flattened into a slight transverse expansion and two weak condyles. The radius is straight except for the slightly medially curved proximal end, and is thinner than the ulna. The articular surface of the proximal end is nearly oval.

The flat carpal bones (ulnare, intermedium, and distal carpal 2) are preserved in IVPP-V11797-18 (Fig. 16B). The

Table 3. Lengths (in mm) of forelimb elements in the holotype of *Sinornithomimus dongi* gen. et sp. nov. (IVPP-V11797-10). Asterisks indicate minimum lengths.

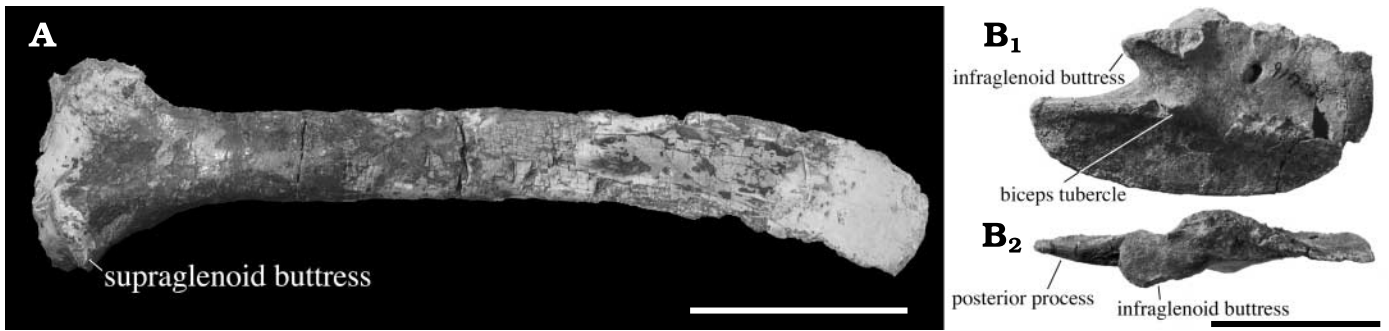|			
Scapula	204	Phalanx I-1	76.3
Coracoid	85.1	Phalanx I-2	–
Humerus	212	Phalanx II-1	19.9
Ulna	147	Phalanx II-2	59.9
Radius	145	Phalanx II-3	48.3*
Metacarpal I	41.2	Phalanx III-1	13.9
Metacarpal II	54.7	Phalanx III-2	14.6
Metacarpal III	53.8	Phalanx III-3	42.9
		Phalanx III-4	46.9*

Fig. 15. **A**. Scapula of *Sinornithomimus dongi* gen. et sp. nov. (IVPP-V11797-10) in lateral view. **B**. Coracoid of IVPP-V11797-20 in lateral (B$_1$) and dorsal (B$_2$) views. Scale bars 5 cm.
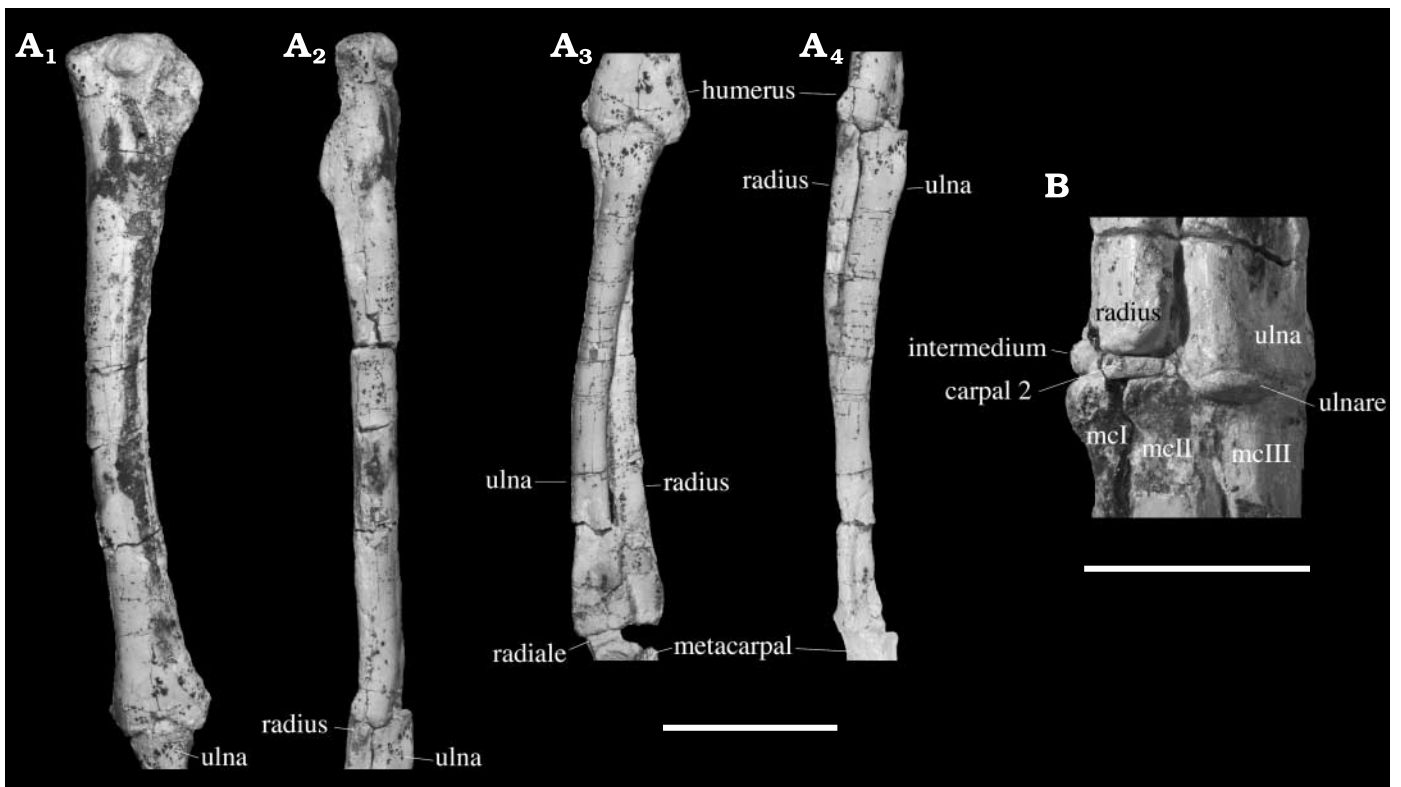

Fig. 16. **A**. *Sinornithomimus dongi* gen. et sp. nov. (IVPP-V11797-10) humerus in dorsal (A$_1$) and lateral (A$_2$) views, and ulna and radius in dorsal (A$_3$) and lateral (A$_4$) views. **B**. Wrist of IVPP-V11797-18 in dorsal view. Scale bars are 3 cm for A and 2 cm for B.

ulnare is thin and fits on the distal end of the ulna. The ulnare and distal carpal 2 are positioned in a similar arrangement to that described in *Struthiomimus altus* (Nicholls and Russell 1985). Distal carpal 2 is relatively smaller than in *Harpymimus okladnikovi*.

All manual digits are subequally developed (Fig. 17). The total length of the manus along metacarpal II and digit II is 170 mm, which is longer than the ulna, unlike in *Gallimimus bullatus*. Using metacarpal II for comparison, the ratio of metacarpals I: II: III is 0.79:1:0.97(Table 3), and this is a derived condition among ornithomimosaurs in having subequal lengths. The distal end of metacarpal I is medially directed and laterally rotated (rotated clockwise for a right hand in distal view). The contact area between metacarpals I and II is

less than a half of the length of metacarpal I. The distal end of this contact is associated with a ridge along the medial border of metacarpal I. Metacarpal I has two distal condyles, forming a ginglymoid articulation, but the lateral one is reduced as in *Archaeornithomimus asiaticus*. Metacarpal II has weakly developed distal condyles separated by a shallow sulcus. Metacarpal III has a short contact surface at its proximal end with metacarpal II. The distal end has a spherical main condyle for articulation with phalanx III-1 and has two small condyles on the posterior surface.

The manual phalangeal formula is 2-3-4-0-0 (Figs. 17, 18). Phalanx I-1 is the longest among the hand elements and is longer than the sum of lengths of phalanges III-1 and III-2 (Table 3) as in other ornithomimosaurs (Barsbold and Osmólska
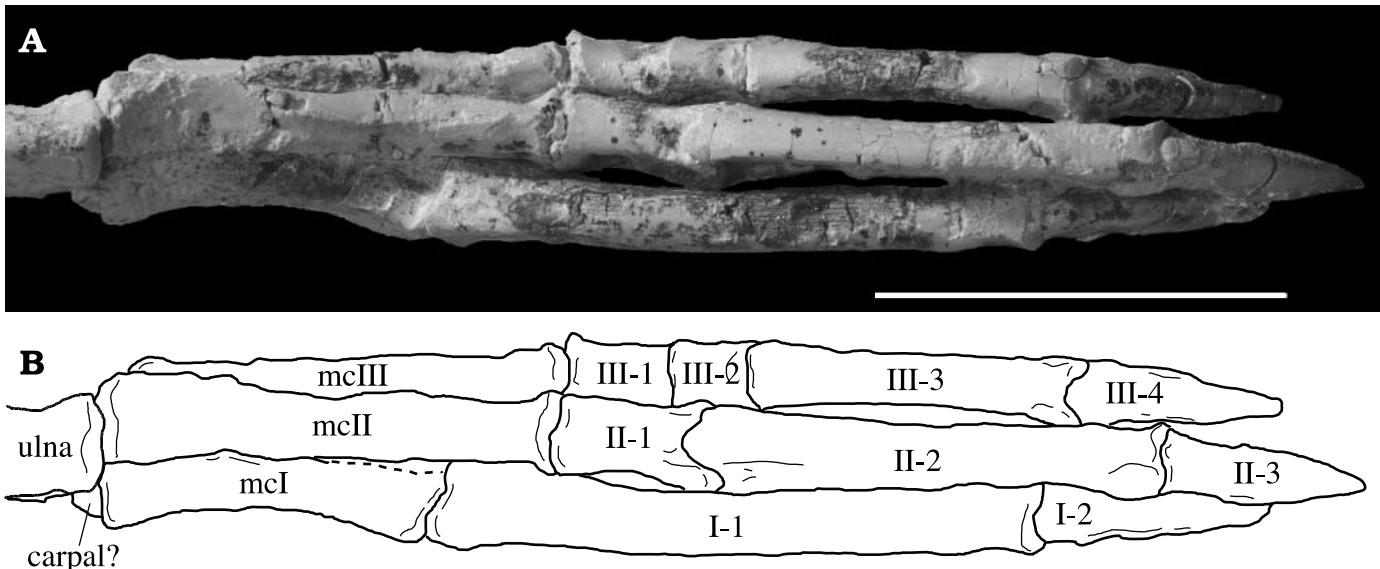
Fig. 17. Left hand of *Sinornithomimus dongi* gen. et sp. nov. (IVPP-V11797-10) in dorsal view. Photograph (**A**) and explanatory drawing of the same (**B**). Scale bar 5 cm.

1990; Pérez-Moreno et al. 1994). Phalanx I-1 is more than three times longer than phalanx II-1 and is approximately five times longer than phalanx III-1 (2.5 times and 3.5 times, respectively, in *Gallimimus bullatus*; Osmólska et al. 1972). Phalanx I-1 is the only most-proximal phalanx that has a proximal dorsal process, as found in the penultimate phalanges, which fits in an intercondylar groove on the dorsal surface of metacarpal I. The penultimate phalanges are similar in shape and have ginglymoid articulations. The shafts of the penultimate phalanges of digits I and II are dorsally curved in lateral view, but of digit III is nearly straight (Fig. 18). Phalanges II-1, III-1, and III-2 are distinguishable from the penultimate phalanges in having nearly parallel lateral borders in dorsal view, faint lateral ligament fossae, depressed ventral surfaces distally, and deep sulci between the distal condyles. The proximal articular surface of phalanx III-2 is distinctly divided by a ridge, differing from the single depression in phalanges II-1 and III-1. The ungual phalanges are laterally compressed with medial and lateral grooves. The flexor tubercles for the tendons of M. flexor profundus are distally placed and are as developed as in *Gallimimus bullatus* (Osmólska et al. 1972: fig. 14). All of the ungual phalanges are weakly curved in lateral view, but the ungual of digit I has the strongest curvature.

The length of the ilium (Fig. 19A) is slightly less than that of the pubis (Table 4), and is more than twice as long as the iliac height above the center of acetabulum. The height of the ilium decreases posterior to the ischial peduncle. A ventrally directed process on the anteroventral portion of the antilium is present as in other ornithomimosaurs, although its pointed tip is missing in all specimens. The pubic peduncle is much stronger than the ischial peduncle. The ischial peduncle is triangular with a ventrally pointing apex in lateral view. The ventral end is anteroposteriorly flattened, for a peg-and-socket articulation. The lateral edge of the supraacetabular crest has a lateral expansion. The ilia in IVPP-11797-11

nearly meet each other along all of the dorsal edge except near the posterior portion, where they diverge.

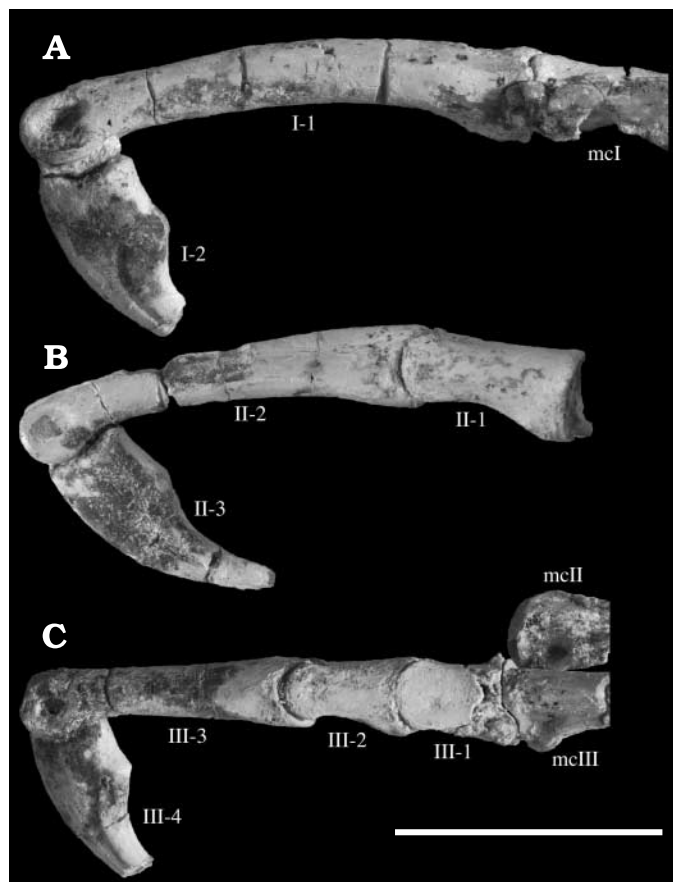The pubis (Fig. 19B) has a straight shaft with an anteroposteriorly-expanded boot at the distal end. The ventral mar-

Fig. 18. Left manual digits of *Sinornithomimus dongi* gen. et sp. nov. (IVPP-V11797-18) in lateral view. Digit I (**A**), digit II (**B**), and digit III (**C**). Scale bar 5 cm.
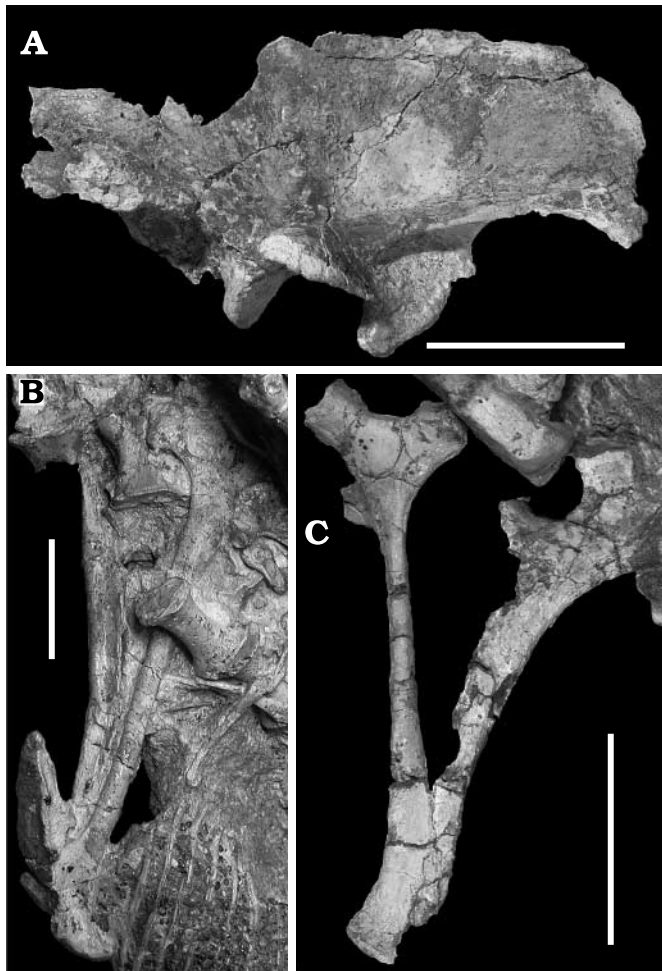
Figure 19. Pelvic girdle elements of *Sinornithomimus dongi* gen. et sp. nov. Right ilium of IVPP-V11797-10 in lateral view (**A**), pubes of IVPP-V11797-9 in posterolateral view (**B**), and ischia of IVPP-V11797-15 in lateral view (**C**). Scale bars 5 cm.

Table 4. Proximodistal lengths (in mm) of pelvic girdle and hindlimb elements in the holotype of *Sinornithomimus dongi* gen. et sp. nov. (IVPP-V11797-10). Ilium length and height is anteroposteriorly and dorsoventrally, respectively.

Ilium length and height	268 X 112	Phalanx II-2	26.7
Pubis	330	Phalanx II-3	38.9
Ischium	236	Phalanx III-1	50.3
Femur	323	Phalanx III-2	39.6
Tibiotarsus	347	Phalanx III-3	30.0
Tibia	335	Phalanx III-4	35.5
Fibula	323	Phalanx IV-1	25.6
Astragalus width	48.6	Phalanx IV-2	21.8
Calcaneum	15.8	Phalanx IV-3	14.5
Metatarsal III	213.0	Phalanx IV-4	12.1
Metatarsal IV	197.2	Phalanx IV-5	31.2
Metatarsal V	82.4		

accessory trochanter. The weakly developed fourth trochanter is positioned at one-third of the femur length from the proximal end and is slightly stronger than in *Garudimimus brevipes* and *Gallimimus bullatus*. On the posterior surface of the lateral distal condyle, a protuberance extends posteriorly and bends laterally unlike *Garudimimus brevipes*.

The tibia (Figs. 20, 22) is the longest of the hindlimb elements. The cnemial crest, positioned on the anterior side of the proximal end, curves laterally. Along the lateral surface of the upper third of the proximal tibial shaft the crest contacts the fibula. The anterior surface of the distal end is flat with a shallow groove for the fibula. Unlike *Harpymimus okladnikovi* and *Garudimimus brevipes*, the posterolateral
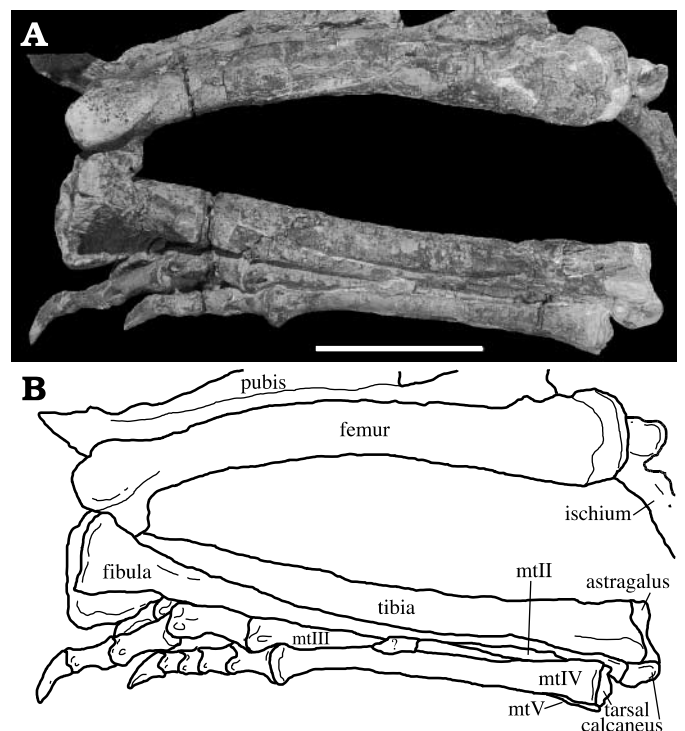

Fig. 20. Left hindlimb of *Sinornithomimus dongi* gen. et sp. nov. (IVPP-V11797-10) in lateral view. Photograph (**A**) and explanatory drawing of the same (**B**). Scale bars 5 cm.
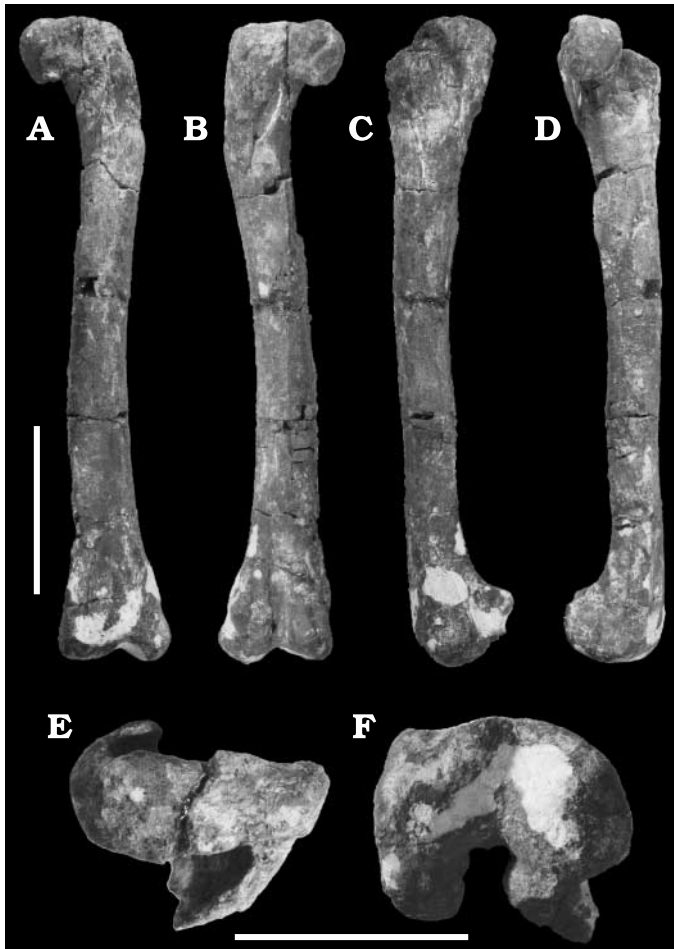
gin of the boot is faintly concave in lateral view. The anterior extension of the boot is more rounded and shorter than the posterior one. The angle between the pubic shaft and the anteroposterior axis of the boot is 65 degrees, whereas it is 50 degrees in *Gallimimus bullatus*. The pubis has an apron along the medial surface of the pubic shaft beginning about one–third of the length from the proximal end of the pubis (110 mm) to the pubic boot.

The ischium (Fig. 19C) is as slender as the pubis and roughly two-thirds of the pubic length (Table 4). The iliac peduncle is stronger than the pubic peduncle. The sutural surface of the iliac peduncle is excavated, to receive the ischial peduncle of the ilium. The ischial shaft is nearly straight and has an apron formed by the obturator process on its medial surface. The distal end is slightly wider than the shaft.

The femur (Figs. 20, 21) is slightly shorter than the tibia (Table 4). It has a wing-like lesser trochanter, which is lower than the femur head, and is separated from the femur head by a deep notch. The anterior border of the lesser trochanter has an

Fig. 21. Left femur of *Sinornithomimus dongi* gen. et sp. nov. (IVPP-V11797-23) in anterior (**A**), posterior (**B**), lateral (**C**), medial (**D**), proximal (**E**), and distal (**F**) views. Scale bars 5 cm for A–D, and 2 cm for E and F.

corner of the distal tibia lacks a ridge. The slender fibula has a proximal end that is more than six times wider than the shaft at the mid-length, whereas it is only five times wider in *Ornithomimus edmontonicus* Sternberg, 1933 (Parks 1933). The medial side of the fibula has a depression, positioned close to its proximal end as in other ornithomimosaurs and tyrannosaurs.

The astragalus (Fig. 22) is firmly attached to the tibia. The anterior ascending process is triangular in anterior view and extends proximally slightly less than in *Gallimimus bullatus* (the ratio of astragalus to tibiotarsus length is 0.22 in *Sinornithomimus dongi* and 0.25 in *Gallimimus bullatus*) (Osmólska et al. 1972). The lateral border of the astragalus has a notch for a prominence of the calcaneus. The reduced calcaneus contacts the fibula, the tibia and the lateral surface of the astragalus.

Two flat distal tarsals (III and IV) are similar to those in *Archaeornithomimus asiaticus* (Gilmore 1933) and *Gallimimus bullatus* (Osmólska et al. 1972) in that distal tarsal III is smaller than IV and sits on the posterior part of the proximal surface of metatarsals II and III. Distal tarsal IV primarily con-

tacts metatarsal IV. Metatarsal III is not completely covered and is more exposed than in *Archaeornithomimus asiaticus*.

The metatarsals (Fig. 23) are sub-equal in length and show the arctometatarsalian condition. The proximal end of metatarsal III narrows rapidly and is invisible in the anterior view. Metatarsals II and IV contact each other proximally. The lateral surface of metatarsal II and the medial surface of metatarsal IV are concave for the proximal end of metatarsal III. The length of metatarsal III is 69% that of the femur, which is less than in *Gallimimus bullatus* (80%) and *Dromiceiomimus brevitertius* (86%) (Osmólska et al. 1972; Barsbold and Osmólska 1990) but is similar to *Garudimimus brevipes* (60%). Unlike *Harpymimus okladnikovi* and *Garudimimus brevipes*, the lateral ligament fossae are deep except on the medial surface of metatarsal II and the lateral surface of metatarsal IV. Metatarsal V, positioned on the plantar side, is thin and reduced in size with a uniform width.

The pedal phalangeal formula is 0-3-4-5-0 as in other ornithomimosaurs (Fig. 24) except *Garudimimus brevipes* in
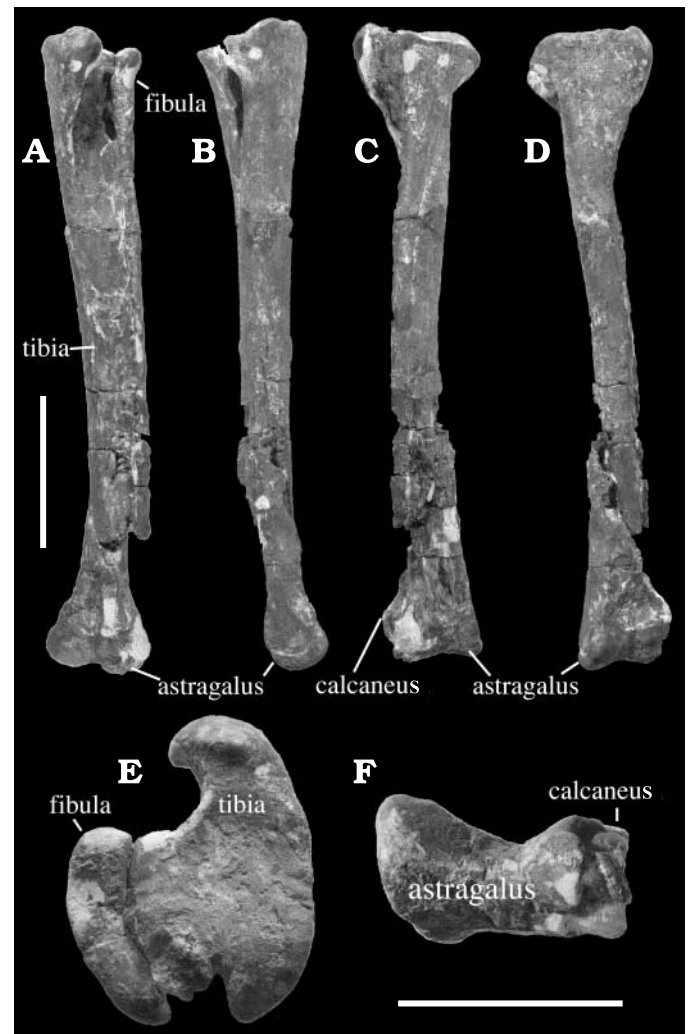

Fig. 22. Left tibiofibularis with tarsals of *Sinornithomimus dongi* gen. et sp. nov. (IVPP-V11797-23) in anterior (**A**), posterior (**B**), lateral (**C**), medial (**D**), proximal (**E**), and distal (**F**) views (distal one-fourth is crushed and displaced). Scale bars 5 cm for A–D, and 2 cm for E and F.
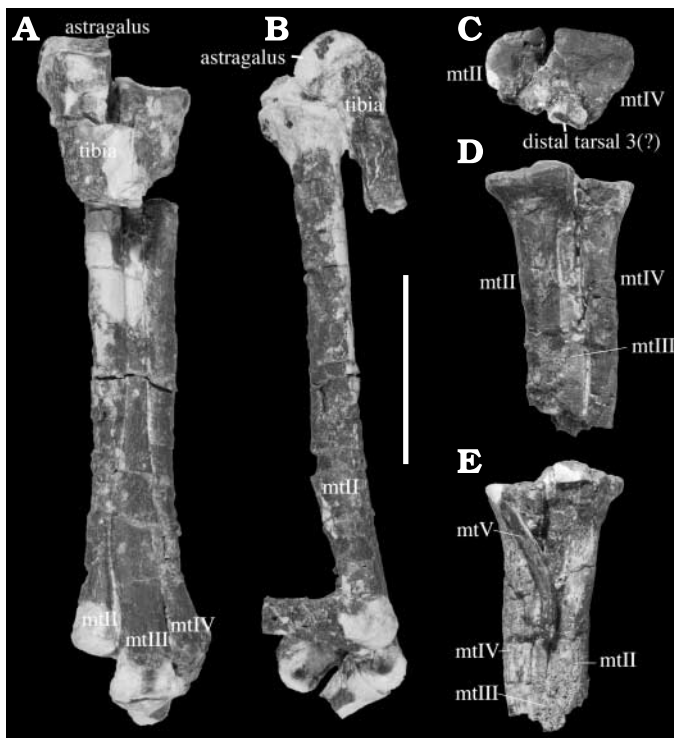
Fig. 23. Left metatarsals of *Sinornithomimus dongi* gen. et sp. nov. (IVPP-V11797-23) in anterior (**A**) and medial (**B**) views. IVPP-V11797-25 in proximal (**C**), anterior (**B**), posterior (**E**) views. Scale bar 5 cm.
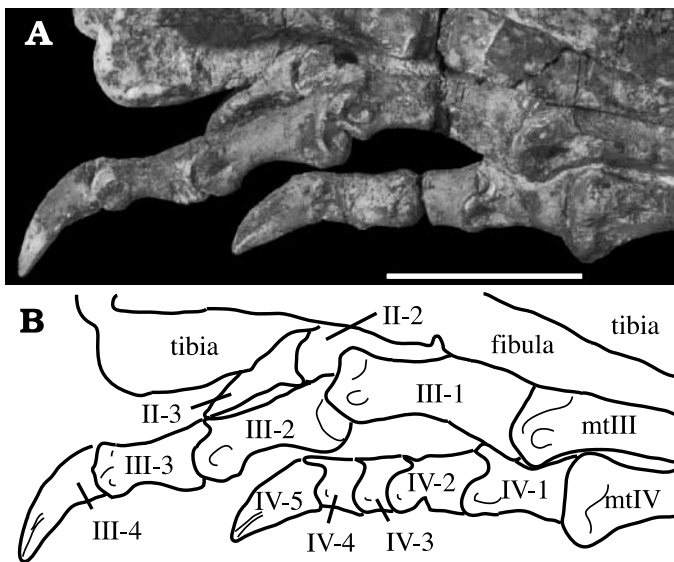

Fig. 24. Left pedal digits of *Sinornithomimus dongi* gen. et sp. nov. in IVPP-V11797-10 in lateral view. Photograph (**A**) and explanatory drawing of the same (**B**). Scale bar 5 cm.

which digit I is present (Barsbold 1981). Digit III is the longest, and digit IV is the shortest. The proximal articular surfaces of all of the most proximal phalanges are shallowly concave and undivided. The articular surfaces between the phalanges in digits II and IV are divided asymmetrically by low ridges on the proximal surfaces and by grooves on the

distal ends. The phalanges of digit III lack ginglymoid articulations except for the ungual-penultimate articulation. The unguals of digits II and IV are directed anteromedially and anterolaterally, respectively, with respect to the sagittal plane of the foot in dorsal view. As in other ornithomimids, the ventral surfaces of the unguals are flat and the posterior part of each surface has a depression with a weak longitudinal ridge but no tuber.

Discussion

Behaviour and ontogeny.—At least fourteen individuals are present in the Ulan Suhai locality. Most skeletons are of juveniles (Table 5), but there are three large individuals (IVPP-V11797-10, -19, and -29). An isolated ulna (IVPP-V11797-19) is 24.6 cm long (missing the proximal tip of the olecranon process). Excluding the olecranon process its length is 23.6 cm, close to the radius length of IVPP-V11797-19. Based on an allometric equation derived from data in Table 5 (radius vs. femur length), the femur length of IVPP-V11797-19 is estimated to be 48 cm [(radius length) = 0.1248 (femur length)[1.2217]]. Its estimated femur length is much larger than that of IVPP-V11797-29 (41.3 cm). The ratio of (ulna of IVPP-V11797-19)/ (femur of IVPP-V11797-29) is 59.6%, which is much larger than the ulna/femur ratio in IVPP-V11797-10 and exceeds the range of the ulna/femur ratios (38 to 53%) known in ornithomimids (Nicholls and Russell 1981). Although the forelimb/femur ratio changes with growth in *Sinornithomimus dongi*, IVPP-V11797-19 is probably larger than IVPP-V11797-29 and is the largest individual from the Ulan Suhai locality.

Nearly complete, articulated skeletons of *Sinornithomimus dongi* were recovered from a single horizon as a mono-specific bonebed. The preservation of all skeletons is uniform, and bone surfaces show no weathering features (no cracks or fractures) or tooth marks, suggesting that the ornithomimids suffered a single mass mortality event and were buried simultaneously with relatively short exposure to the elements, and without being scavenged. The distribution of femur lengths (Table 5) demonstrates the relatively large population of juveniles, ranging from 16.5 to 21 cm, although there are two large individuals (33 and 41 cm). With the exclusion of these large individuals, a histogram shows a highly kurtose, but symmetrical distribution, indicating that these juveniles are similar in age (Fig. 26). This size distribution differs from that in other theropod bonebeds (e.g., *Coelophysis*, *Allosaurus*, and *Albertosaurus*), which have a variety of ontogenetic stages (Horner 1997; Currie 1998). Numerous juveniles with a few adults from a bonebed suggest attritional (or selective) mortality for juveniles or a catastrophic (non-selective) mass mortality with a high proportion of juveniles in the living population (Varricchio and Horner 1993). The bonebeds of the hadrosaur *Maiasaura* show a similar size distribution profile to the *Sinornithomimus dongi* bonebed, and the *Maiasaura* bonebeds are in-
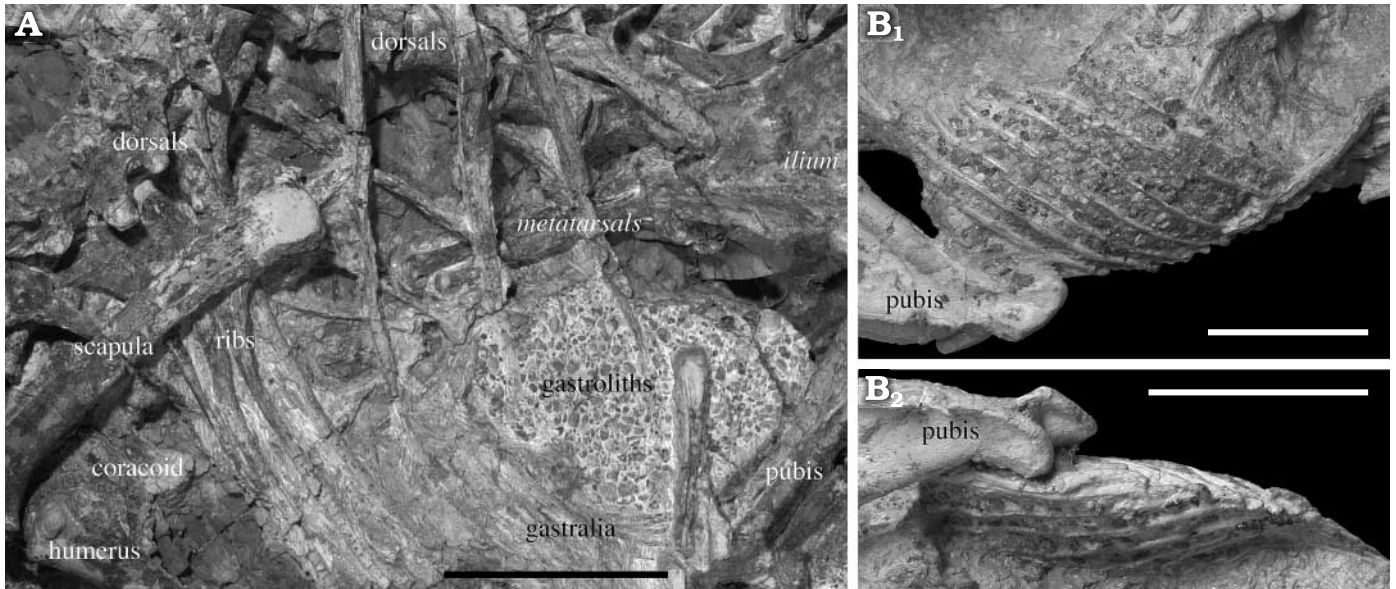
Fig. 25. **A**. Gastrolith masses of *Sinornithomimus dongi* gen. et sp. nov. IVPP-V11797-10 in lateral view. **B**. IVPP-V11797-9 in lateral (B₁) and ventral (B₂) views. Italicized letters in A indicate disarticulated and isolated elements not from IVPP-V11797-10. Scale bars 10 cm for A and 5 cm for B.

terpreted as nesting sites (Horner and Makela 1979; Horner 1994; Varricchio and Horner 1993). However, the probability that the skeletons of *Sinornithomimus dongi* were in proximity to a nesting site is unlikely, because no evidence of nesting behavior (nests, eggshells, and remains of hatchlings) has been found. Furthermore, all juveniles are mature enough to travel with the adults (inferred from well formed articular surfaces on limb bones). Although it is not clear what caused the mortality of *Sinornithomimus dongi* or if the bonebed reflects attritional or catastrophic mortality, the accumulation clearly suggests that *Sinornithomimus dongi* exhibited gregarious behavior with a large number of juveniles. Because *Sinornithomimus dongi* is probably an herbivorous dinosaur (Kobayashi et al. 1999), it is plausible that it formed

Table 5. Lengths (in mm) and ratios of selected parts of the skeletons of *Sinornithomimus dongi* gen. et sp. nov. in order of femur length. Abbreviations: Ant, anteroposterior length of the antorbital fossa; Fe, femur length; Hu, humerus length; Ra, radius length; Sk, anteroposterior length of skull; and Ti, tibia length.

Specimen number	Fe	Sk	Sk/Fe	Ant/Sk	Hu/Fe	Ra/Fe	Ti/Fe
IVPP-V11797-2	165	–	–	–	–	–	–
IVPP-V11797-12	178	–	–	–	0.608	0.408	0.995
IVPP-V11797-15	181	–	–	–	0.549	0.375	0.997
IVPP-V11797-14	184	–	–	–	0.553	–	–
IVPP-V11797-23	190	–	–	–	–	–	–
IVPP-V11797-1	193	–	–	–	–	–	–
IVPP-V11797-9	194	–	–	–	–	–	–
IVPP-V11797-13	195	–	–	–	–	0.409	1.024
IVPP-V11797-11	200	130.6	0.634	0.514	0.601	–	1.026
IVPP-V11797-22	201	–	–	–	–	–	–
IVPP-V11797-3	212	–	–	–	–	–	–
IVPP-V11797-10	323	183.1	0.567	0.582	0.656	0.449	1.037
IVPP-V11797-29	413	–	–	–	–	–	1.068

herds for protection from predators, similar to other herbivorous dinosaurs.

Ontogenetic variation in *Sinornithomimus dongi* is comparable to that in *Gallimimus bullatus* (Osmólska et al. 1972) including the decrease in the ratio of skull length to femur length and increases in the ratios of antorbital region of skull to skull length and radius length to femur length with growth (Table 5). The ratio of humerus length to femur length in *Sinornithomimus dongi* is greater in larger individuals. The increases in the humerus and radius with respect to the femur length indicate the relative elongation of forelimb though ontogeny. Previous studies (Osmólska et al. 1972; Russell 1972; Nicholls and Russell 1981) suggested little change in limb proportions in ornithomimid ontogeny. However,
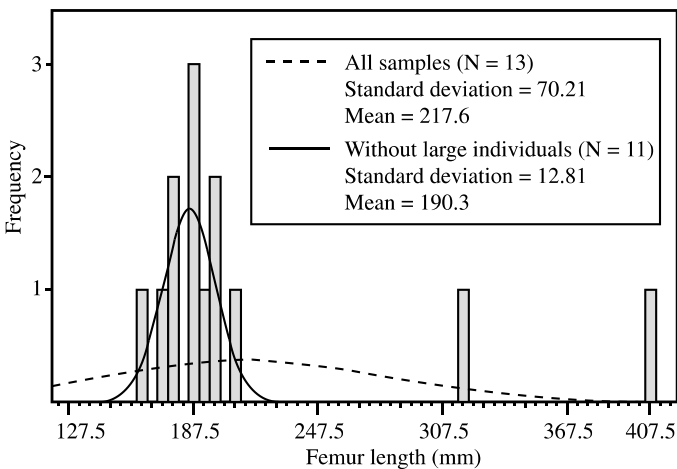

Fig. 26. Histogram of femur lengths of *Sinornithomimus dongi* gen. et sp. nov. (Table 5). Kurtotic distribution curves are drawn for all samples (dashed line) and for juveniles (solid line).

Sinornithomimus dongi demonstrates an increase in the relative ratio of the tibia to femur. Currie (1998) compared the lengths of limb elements of tyrannosaurids with ornithomimids and suggested a similarity between ornithomimids and juvenile tyrannosaurids indicating greater cursoriality in juvenile tyrannosaurids. In contrast, the change in tibia/femur ratio in *Sinornithomimus dongi* suggests that adult ornithomimids may have been better adapted for fast running than juveniles.

Phylogenetic analysis and comparisons.—Thirty-eight characters (17 cranial and 21 postcranial) were employed in a phylogenetic analysis of Ornithomimosauria (Appendix 1). All characters are equally weighted and unordered. Most characters are coded as binary, only two (26 and 28) as multistate. Ten ornithomimosaurian in-group taxa and two outgroups, *Allosaurus* and tyrannosaurids, were used, and characters for all terminal taxa are obtained from literature or specimens listed in Table 6. The data matrix (Appendix 2) was analyzed using PAUP 4.0Beta (Swofford 2000), with Branch-and-Bound search. The analysis produced a single most parsimonious tree of 58 steps, with C.I.= 0.690, R.I.= 0.747, and R.C.= 0.515 (Fig. 27).

In the cladogram recovered by the present analysis, *Sinornithomimus* is positioned within Ornithomimidae as suggested by Kobayashi et al. (2001). The general tree topology is similar to one for Ornithomimosauria by Osmólska (1997) except for the relationships of *Pelecanimimus*, *Harpymimus*, *Gallimimus*, and *Anserimimus*. The monophyly of Ornithomimidae has been supported previously by a
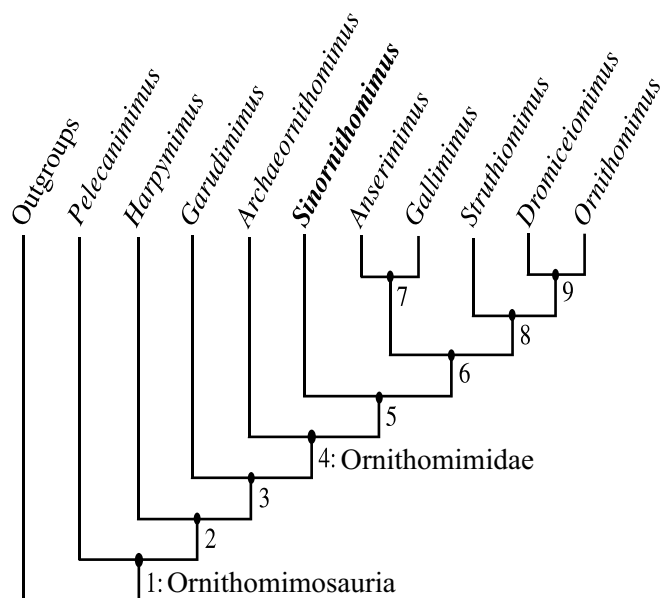

Fig. 27. The single most parsimonious tree of Ornithomimosauria. Synapomorphies for each node (ACCTRAN/DELTAN): Node 1 (5(0), 8, 11, 13, 15, 17, 18, 20, 22, 25, 28, 29, 31, 32, 33/ 8, 11, 18, 20, 25, 32, 33); Node 2 (1, 3, 6, 9, 16/ 1, 3, 5, 6, 9, 13, 16, 17, 22); Node 3 (2, 7, 10, 12, 14, 26(2), 38/ 2, 7, 10, 12, 38); Node 4 (15(0), 36, 37/ 26(2), 28, 29, 31, 37); Node 5 (19/ 19, 36); Node 6 (30/ 30); Node 7 (14(0), 16(0), 17(0), 21, 23, 27/ 21, 23); Node 8 (5, 35/ 5, 14, 35); Node 9 (22(0), 24, 28(2)/ 22(0), 24). See Appendix 1 for list of characters.

number of characters (Barsbold and Osmólska 1990). However, the presented phylogenetic analysis suggests that there is only one unambiguous synapomorphy (arctometatarsalian condition) for the family, which was also noted by Norell et al. (2002). Some characters previously considered as ornithomimid synapomorphies are in fact plesiomorphic. Although the arctometatarsalian condition was proposed as a synapomorphy of Arctometatarsalia (Tyrannosauridae plus Ornithomimidae, and possibly Troodontidae) by Holtz (1994, 1998), the condition was derived convergently within Ornithomimosauria and is an important character for the clade of Ornithomimidae.

The ginglymoid distal condyles of metacarpal I in *Sinornithomimus* suggest that *Sinornithomimus* is basal to the clade of *Anserimimus*, *Gallimimus*, and North American taxa (*Struthiomimus*, *Dromiceiomimus*, and *Ornithomimus*) but is more derived than *Archaeornithomimus*, because of a low ratio of the anteroposterior lengths of the cervical neural spines compared with neural arch lengths. The condition of the ginglymoid metacarpal-phalangeal articulation in *Sinornithomimus* is similar to that of *Archaeornithomimus*, but different from that of *Harpymimus* in having a reduced medial condyle. Pérez-Moreno and Sanz (1995) suggested two states in the ornithomimosaur hand structure based on the orientation of metacarpal I's distal end (medially directed or parallel to metacarpal II), but metacarpal I in most taxa is medially directed to some degree depending on the position of initial medial divergence. The distribution of characters related to metacarpal I in our phylogeny indicate that there are three states in ornithomimosaur hand structure. The first, seen in *Harpymimus,* is the primitive condition (short metacarpal I, medially rotated distal end, and strong ginglymoid metacarpal-phalangeal articulation). *Sinornithomimus* and *Archaeornithomimus* show the second state, with subequal metacarpals I and II, laterally rotated distal ends and ginglymoid articulations with reduced medial condyles. The clade of *Anserimimus*, *Gallimimus*, and North American taxa share a bowl-shaped metacarpal-phalangeal articulation with even greater reduction of the medial condyle (third state). The functional implication of this model is that primitive ornithomimosaur hands are more "raptorial" and had a better capability of grasping as in other theropods than derived forms, which were adapted for hooking and clamping as discussed by Nicholls and Russell (1985). *Pelecanimimus* exhibits the second stage (Pérez-Moreno and Sanz 1995). Although it is basal to *Harpymimus* in our cladogram, our phylogenetic analysis indicates the derived manus structure of *Pelecanimimus* is convergent because *Harpymimus* is more derived than *Pelecanimimus* based on cranial characters (1, 3, 6, 9, and 16 in Appendix 1).

Our phylogenetic analysis suggests two clades for Late Cretaceous ornithomimids (Mongolian and North American ornithomimid clades). Two characters (arrangements of biceps tubercle and glenoid in the scapula and coracoid) support monophyly of *Anserimimus* and *Gallimimus*. Both genera are known from the Nemegt Formation, but their mono-

Table 6. Specimens and literature used for phylogenetic analysis.

Taxon	Source
Allosaurus *Allosaurus fragilis* Marsh, 1877	Madsen 1976
Tyrannosauridae *Tyrannosaurus rex* Osborn, 1905 *Albertosaurus libratus* (Lambe, 1914) *Daspletosaurus torosus* Russell, 1970	Osborn 1905; Osborn 1916; Bakker et al. 1988; Carr 1999 Carr 1999 Russell, 1970; Carr 1999
Pelecanimimus *Pelecanimimus polyodon* Pérez-Moreno, Sanz, Buscalioni, Moratalla, Ortega, and Rasskin-Gutman, 1994	Pérez-Moreno et al. 1994
Harpymimus *Harpymimus okladnikovi* Barsbold and Perle, 1984	GIN 100/29; Barsbold and Perle 1984
Garudimimus *Garudimimus brevipes* Barsbold, 1981	GIN 100/13; Barsbold 1981
Archaeornithomimus *Archaeornithomimus asiaticus* (Gilmore, 1933)	AMNH 6565-6559, AMNH 21797, AMNH 21779-21801, AMNH 21803, AMNH 21884-21892; Gilmore 1933; Smith and Galton 1990
Anserimimus *Anserimimus planinychus* Barsbold, 1988	GIN 100/300; Barsbold 1988
Gallimimus *Gallimimus bullatus* Osmólska, Roniewicz, and Barsbold, 1972 *Gallimimus* sp.	GIN 100/10, GIN 100/11, GIN 100/12, GIN 100/1133; Osmólska et al. 1972 GIN 950818, GIN 100/14
Ornithomimus *Ornithomimus velox* Marsh, 1890 *Ornithomimus edmontonicus* Sternberg, 1933 *Ornithomimus* sp.	Marsh 1890; DeCourten and Russell 1985 ROM 851; Sternberg 1933; Parks 1933; Russell 1972 TMP 95.110.1, TMP 93.62.1
Dromiceiomimus *Dromiceiomimus brevitertius* (Parks, 1926) *Dromiceiomimus samueli* (Parks, 1928)	ROM 797, ROM 852; Parks 1926; Russell 1972 ROM 840; Parks 1928; Russell 1972
Struthiomimus *Struthiomimus altus* Lambe, 1902 *Struthiomimus* sp.	ROM 1790, UCMZ(VP)1980.1; Osborn 1916; Russell 1972; Nicholls and Russell 1985 TMP 90.26.1

phyletic relationship has never been proposed previously. The more anteriorly positioned biceps tubercle of the coracoid in *Anserimimus* and *Gallimimus* suggests more anteriorly directed muscle pull (M. biceps brachii) relative to the glenoid than other ornithomimosaurs (Nicholls and Russell 1985) and may be related to the lateral displacement of the glenoid (more laterally facing glenoid than other ornithomimosaurs).

Monophyly of the North American taxa (*Struthiomimus*, *Dromiceiomimus*, and *Ornithomimus*) is characterized by the ventral expansion of the pubic boot and the presence of a series of maxillary neurovascular foramina. Changes in character state of the latter feature imply a possible evolutionary pattern in the structure of a rhamphotheca. All ornithomimosaurs except *Pelecanimimus* have gaps in the anterior rostrum created by the ventrally curved dentaries, but the gaps were closed by a rhamphotheca as preserved in *Ornithomimus* and *Gallimimus* (Norell et al. 2001). Interestingly, foramina are absent from the maxilla of *Sinornithomimus* and *Gallimimus* (also maybe absent in *Harpymimus* and *Garudimimus* although further preparation is required), but are present in *Struthiomimus* and *Ornithomimus* (foramina are present in the premaxilla in all taxa). If the distribution of foramina in the premaxilla and maxilla is associated with the formation of a rhamphotheca, a rhamphotheca on the upper jaw evolved prior to that of the lower jaw as exemplified in *Harpymimus* (which has foramina for nourishing a rhamphotheca in the premaxillae but teeth in the dentaries). The area covered by a rhamphotheca in the rostrum of the North American taxa is larger than in Asian forms, indicating different feeding or display adaptations. The anterior ends of the premaxillae in North American taxa are acute, whereas those of Asian forms are U-shaped in dorsal view (Makovicky et al. in press). This feature may demonstrate a real difference in beak morphology between North American and Asian taxa.

Acknowledgements

References

Bakker, R.T., Williams, M., and Currie, P.J. 1988. *Nanotyrannus*, a new genus of pygmy tyrannosaur from the latest Cretaceous of Montana. *Hunteria* 1: 1–30.

Barsbold, R. 1976. On the evolution and systematics of the late Mesozoic dinosaurs [in Russian]. *In*: N.N. Kramarenko (ed.), Paleontologiâ i biostratigrafiâ Mongolii. *Sovmestnaâ Sovetsko-Mongolskaâ Paleontologičeskaâ Ekspediciâ, Trudy* 3: 3: 68–75.

Barsbold, R. 1981. Toothless carnivorous dinosaurs of Mongolia [in Russian]. *Sovmestnaâ Sovetsko-Mongolskaâ Paleontologičeskaâ Ekspediciâ, Trudy* 15: 28–39.

Barsbold, R. 1988. A new Late Cretaceous ornithomimid from the Mongolia People's Republic [in Russian]. *Paleontologičeskij žurnal* 1988 (1): 122–125.

Barsbold, R. and Osmólska, H. 1990. Ornithomimosauria. *In*: D.B. Weishampel, P. Dodson, and H. Osmólska (eds.), *The Dinosauria*, 225–244. University of California Press, Berkeley.

Barsbold, R. and Perle, A. 1984. On first new find of a primitive ornithomimosaur from the Cretaceous of the MPR [in Russian]. *Paleontologičeskij žurnal* 1984 (2): 121–123.

Bureau of Geology and Mineral Resources of Nei Mongol Autonomous Region. 1991. Regional geology of Nei Mongol (Inner Mongolia) Autonomous Region. *People's Republic of China Ministry of Geology and Mineral Resources, Geological Memoirs* 25: 1–725.

Carr, T.D. 1999. Craniofacial ontogeny in Tyrannosauridae (Dinosauria, Coelurosauria). *Journal of Vertebral Paleontology* 19: 497–520.

Currie, P.J. 1985. Cranial anatomy of *Stenonychosaurus inequalis* (Saurischia: Theropoda) and its bearing on the origin of birds. *Canadian Journal of Earth Sciences* 22: 1643–1658.

Currie, P.J. 1995. New information on the anatomy and relationships of *Dromaeosaurus albertensis* (Dinosauria: Theropoda). *Journal of Vertebral Paleontology* 15: 576–591.

Currie, P.J. 1998. Possible evidence of gregarious behavior in tyrannosaurids. *GAIA* 15: 271–277.

DeCourten, F.L. and Russell, D.A. 1985. A specimen of *Ornithomimus velox* (Theropoda, Ornithomimidae) from the terminal Cretaceous Kaiparowits Formation of southern Utah. *Journal of Paleontology* 59: 1091–1099.

Gilmore, C. W. 1933. On the dinosaurian fauna of the Iren Dabasu Formation. *Bulletin of the American Museum of Natural History* 67: 23–78.

Godefroit, P., Dong, Z.-M., Bultynck, P., Li, H., and Feng, L. 1998. Sino-Belgian Cooperation Program, Cretaceous dinosaurs and mammals from Inner Mongolia. 1. New *Bactrosaurus* (Dinosauria: Hadrosauroidea) material from Iren Dabasu (Inner Mongolia, P.R. China). *Bulletin de l'Institut Royal des Sciences Naturelles de Belgique* 68: 1–70.

Head, J.J. 2001. A reanalysis of the phylogenetic position of *Eolambia caroljonesa* (Dinosauria, Iguanodontia). *Journal of Vertebrate Paleontology* 21: 392–396.

Holtz, T.R., Jr. 1994. The phylogenetic position of the Tyrannosauridae: implications for theropod systematics. *Journal of Paleontology* 68: 1100–1117.

Holtz, T.R., Jr. 1998. A new phylogeny of the carnivorous dinosaurs. *GAIA* 15: 5–61.

Horner, J.R. 1994. Comparative taphonomy of some dinosaur and extant bird colonial nesting grounds. *In*: K. Carpenter, K.F. Hirsch, and J.R. Horner (eds.), *Dinosaur Eggs and Babies*, 116–123. Cambridge University Press, Cambridge.

Horner, J.R. 1997. Behavior. *In*: P.J. Currie and K. Padian (eds.), *Encyclopedia of Dinosaurs*, 45–50. Academic Press, San Diego.

Horner, J.R. and Makela, R. 1979. Nest of juveniles provides evidence of family structure among dinosaurs. *Nature* 282: 296–298.

Hurum, J.H. 2001. Lower jaw of *Gallimimus bullatus*. *In*: D.H. Tanke and K. Carpenter (eds.), *Mesozoic Vertebrate Life*, 34–41. Indiana University Press, Bloomington.

Kobayashi, Y., Lü, J.-C., Dong, Z.-M., Barsbold, R., Azuma, Y., and Tomida, Y. 1999. Herbivorous diet in an ornithomimid dinosaur. *Nature* 402: 480–481.

Kobayashi, Y., Lü, J.-C., Azuma, Y., Dong, Z.-M., and Barsbold, R. 2001. Bonebed of a new gastrolith-bearing ornithomimid dinosaur from the Upper Cretaceous Ulansuhai Formation of Nei Mongol Autonomous Region, China. *Journal of Vertebrate Paleontology* 21 (Supplement to 3): 68–69.

Lambe, L.M. 1902. New genera and species from the Belly River Series (mid-Cretaceous). *Geological Survey of Canada, Contributions to Canadian Palaeontology* 3: 25–81.

Lambe, L.M. 1914. On a new genus and species of carnivorous dinosaur from the Belly River Formation of Alberta, with a description of the skull of *Stephanosaurus marginatus* from the same horizon. *The Ottawa Naturalist* 28: 13–20.

Madsen, J.H., Jr. 1976. *Allosaurus fragilis*: a revised osteology. *Utah Geological Survey Bulletin* 109: 1–163.

Makovicky, P. J. 1995. *Phylogenetic aspects of the vertebral morphology of Coelurosauria (Dinosauria: Theropoda)*. Unpublished M.S. dissertation, Copenhagen University, Denmark.

Makovicky, P. J. and Norell, M. A. 1998. A partial ornithomimid braincase from Ukhaa Tolgod (Upper Cretaceous, Mongolia). *American Museum Novitates* 3247: 1–16.

Makovicky, P.J., Kobayashi, Y., and Currie, P.J. (in press). Ornithomimosauria. *In*: D.B. Weishampel, P. Dodson, and H. Osmólska (eds.), *The Dinosauria*, 2nd edition. University of California Press, Berkeley.

Marsh, O.C. 1877. Notice on new dinosaurian reptiles from the Jurassic formation. *The American Journal of Science, Third Series* 14: 514–516.

Marsh, O.C. 1881. Classification of the Dinosauria. *The American Journal of Science, Third Series* 23: 81–86.

Marsh, O.C. 1890. Description of new dinosaurian reptiles. *The American Journal of Science, Third Series* 39: 81–86.

Nicholls, E.L. and Russell, A.P. 1981. A new specimen of *Struthiomimus altus* from Alberta, with comments on the classificatory characters of Upper Cretaceous ornithomimids. *Canadian Journal of Earth Sciences* 18: 518–526.

Nicholls, E.L. and Russell, A.P. 1985. Structure and function of the pectoral girdle and forelimb of *Struthiomimus altus* (Theropoda: Ornithomimidae). *Palaeontology* 28: 643–677.

Norell, M.A., Makovicky, P.J., and Currie, P.J. 2001. The beaks of ostrich dinosaurs. *Nature* 412: 873–874.

Norell, M.A., Clark, J. M., and Makovicky, P. J. 2002. Phylogenetic relationships among coelurosaurian theropods. *In*: J. Gauthier and L.F. Gall (eds.), *New Perspectives on the Origin and Early Evolution of Birds: Proceedings of the International Symposium in Honor of John H. Ostrom*, 49–67. Peabody Museum of Natural History, Yale University, New Haven.

Osborn, H.F. 1905. *Tyrannosaurus* and other Cretaceous carnivorous dinosaurs. *Bulletin of the American Museum of Natural History* 21: 259–265.

Osborn, H.F. 1916. Skeletal adaptation of *Ornitholestes, Struthiomimus, Tyrannosaurus*. *Bulletin of the American Museum of Natural History* 35: 733–771.

Owen, R. 1842. Report on British fossil reptiles, Part II. *Report of the British Association for the Advancement of Science* 11: 60–204.

Osmólska, H. 1997. Ornithomimosauria. *In*: P.J. Currie and K. Padian (eds.), *Encyclopedia of Dinosaurs*, 499–503. Academic Press, San Diego.

Osmólska, H., Roniewicz, E., and Barsbold, R. 1972. A new dinosaur, *Gallimimus bullatus* n. gen., n. sp. (Ornithomimidae) from the Upper Cretaceous of Mongolia. *Palaeontologica Polonica* 27: 103–143.

Padian, K., Hutchinson, J.R., and Holtz, T.R., Jr. 1999. Phylogenetic definitions and nomenclature of the major taxonomic categories of the carnivorous Dinosauria (Theropoda). *Journal of Vertebrate Paleontology* 19: 69–80.

Parks, W. A. 1926. *Struthiomimus brevitertius*, a new species of dinosaur from the Edmonton Formation of Alberta. *Transactions of Royal Society of Canada* 20: 65–70.

Parks, W.A. 1928. *Struthiomimus samueli*, a new species of Ornithomimidae from the Belly Formation of Alberta. *University of Toronto Studies, Geological Series* 26: 1–24.

Parks, W. A. 1933. New species of dinosaurs and turtles from the Upper Cretaceous formations of Alberta. *University of Toronto Studies, Geological Series* 34, 1–33.

Pérez-Moreno, B.P., Sanz, J.L., Buscalioni, A.D., Moratalla, J.J., Ortega, F., and Rasskin-Gutman, D. 1994. A unique multitoothed ornithomimosaur dinosaur from the Lower Cretaceous of Spain. *Nature* 370: 363–367.

Pérez-Moreno, B.P. and Sanz, J.L. 1995. The hand of *Pelecanimimus polyodon*: a preliminary report. *II International Symposium on Lithographic Limestones, Ediciones de la Universidad Autónoma de Madrid (Extended Abstracts)*, 115–117.

Rich, T. H. and Rich, P. V. 1994. Neoceratopsians and ornithomimosaurs: dinosaurs of Gondwana origin? *Research and Exploration* 10: 129–131.

Russell, D.A. 1970. Tyrannosaurs from the Late Cretaceous of western Canada. *National Museum of Natural Sciences Publications in Palaeontology* 1: 1–30.

Russell, D.A. 1972. Ostrich dinosaurs from the Late Cretaceous of western Canada. *Canadian Journal of Earth Sciences* 9: 375–402.

Sereno, P.C. 1998. A rationale for phylogenetic definitions, with application to the higher-level taxonomy of Dinosauria. *Neues Jahrbuch für Geologie und Paläontologie, Abhandlungen* 210: 41–83.

Sereno, P.C. 1999. The evolution of dinosaurs. *Science* 284: 2137–2147.

Smith, D., and Galton, P. 1990. Osteology of *Archaeornithomimus asiaticus* (Upper Cretaceous, Iren Dabasu Formation, People's Republic of China). *Journal of Vertebrate Paleontology* 10: 255–265.

Sternberg, C.M. 1933. A new *Ornithomimus* with complete abdominal cuirass. *Canadian Field-Naturalist* 47: 79–83.

Swofford, D.L. 2000. PAUP*. Phylogenetic analysis using parsimony (*and other methods). Version 4. Sinauer and Associates, Sunderland, Massachusetts.

Varricchio, D.J. and Horner, J.R. 1993. Hadrosaurid and lambeosaurid bone beds from the Upper Cretaceous Two Medicine Formation of Montana: taphonomic and biologic implications. *Canadian Journal of Earth Sciences* 30: 997–1006.

Witmer, L.M. 1997. The evolution of the antorbital cavity of archosaurs: a study in soft-tissue reconstruction in the fossil record with an analysis of the function of pneumaticity. *Journal of Vertebrate Paleontology, Memoir 3* 17 (Supplement to 1): 1–73.

Xu, X., Norell, M. A., Wang, X.-L., Makovicky, P. J., and Wu, X.-C. 2002. A basal troodontid from the Early Cretaceous of China. *Nature* 415: 780–784.

Appendix 1

List of characters used in this study.

1. Premaxillary teeth: present (0) or absent (1) (Holtz 1994).
2. Posterior end of maxillary process of premaxilla terminates anterior to anterior border of antorbital fossa (0) or extends more posteriorly (1).
3. Maxillary teeth: present (0) or absent (1) (Holtz 1994).
4. Maxilla participates in external narial opening (0) or separated from opening by maxilla-nasal contact (1) (Xu et al. 2002).
5. Series of foramina along ventral edge of lateral surface of maxilla: present (0) or absent (1).
6. Prominence on lateral surface of lacrimal: present (0) or absent (1) (Xu et al. 2002).
7. Area of exposed prefrontal in dorsal view: less than that of lacrimal (0) or approximately the same (1) (Xu et al. 2002).
8. Parasphenoid bulla: absent (0) or present (1) (Osmólska et al. 1972).
9. Ventral reflection of anterior portion of dentary, resulting in a gap between upper and lower jaws when jaws are closed: absent (0) or present (1) (Pérez-Moreno et al. 1994).
10. Dentary teeth: present (0) or absent (1) (Holtz 1994).
11. Dentary subtriangular in lateral view (0) or with subparallel dorsal and ventral borders (1) (Currie 1995).
12. Dorsal border of dentary in transverse cross-section: rounded and lacks "cutting edge" (0) or sharp with "cutting edge" (1).
13. Accessory mandibular condyle, lateral to lateral condyle of quadrate: absent (0) or present (1).
14. Foramen on dorsal edge of surangular dorsal to mandibular fenestra: present (0) or absent (1) (Hurum 2001).
15. Posterior surangular foramen: absent (0) or present (1) (Sereno 1999).
16. Number of accessory antorbital fenestra: one (0) or two (1).
17. Mandibular fenestra: heart-shaped with a short and wide process of dentary at anterior part of external mandibular fenestra (0) or oval-shaped without the process (1).
18. Neck length: less (0) or more (1) than twice skull length (Pérez-Moreno et al. 1994).
19. Anteroposterior lengths of cervical neural spines: more (0) or less (1) than one third of neural arch lengths (Makovicky 1995).
20. Posterior process of coracoid: short (0) or long (1) (Pérez-Moreno et al. 1994).
21. Biceps tubercle of coracoid: positioned close to base of posterior process (0) or more anteriorly (1).
22. Depression on dorsal surface of supraglenoid buttress of scapula: present (0) or weak/absent (1) (Nicholls and Russell 1985).
23. Infraglenoid buttress of coracoid: aligned with posterior process (0) or is offset laterally from line of posterior process (1).
24. Robustness of humerus, ratio of width of proximal end to total length: greater (0) or less than 0.2 (1).
25. Deltopectoral crest of humerus: strong (0) or weak (1).
26. Radial condyle of humerus: larger than ulnar condyle (0), approximately equal (1), or smaller (2).
27. Entepicondyle of humerus: weak (0) or strong (1).
28. Length of metacarpal I: approximately half or less than metacarpal II (0), slightly shorter (1) or longer (2) (Russell 1972).
29. Distal end of metacarpal I: medially (0) or laterally (1) rotated (Pérez-Moreno and Sanz 1995).
30. Distal end of metacarpal I forms ginglymoid articulation with distinct condyles (0) or relatively large convex phalangeal articulation with reduced condyles (1) (Pérez-Moreno and Sanz 1995).
31. Metacarpal II: shorter (0) or longer (1) than metacarpal III.
32. First phalanx of manual digit I: shorter (0) or longer (1) than metacarpal II (Pérez-Moreno et al. 1994).
33. Flexor tubercles of manual unguals: positioned at proximal end (0) or distally placed (1) (Nicholls and Russell 1985).
34. Pubic shaft: nearly straight (0) or curved (1) (Norell et al. 2002).
35. Ventral border of pubic boot: nearly straight or slightly convex (0) or strongly convex with ventral expansion (1).
36. First pedal digit: present (0) or absent (1).
37. Proximal end of metatarsal III exposed in anterior view (0) or covered by metatarsals II and IV anteriorly (1) (Norell et al. 2002).
38. Length of pedal phalanx II-2: more than 60% of pedal phalanx II-1 (0) or less (1).

Appendix 2

Data matrix used for phylogenetic analysis of Ornithomimosauria. Missing or unknown characters are represented by "?". Multistate characters are within a parenthesis.

Taxon	5	10	15	20	25	30	35	38
Allosaurus	00000	00000	00000	00000	00000	00000	00000	000
Tyrannosaurids	00010	00000	00000	00000	00000	(12)(01)000	?0000	010
Pelecanimimus	0?0??	0?100	10???	0?1?1	????1	??110	111??	???
Harpymimus	10111	10?10	10101	1110?	01001	10000	0110?	?00
Garudimimus	11111	11111	11111	11?0?	?????	?????	???00	001
Archaeornithomimus	?????	?????	?????	???01	01001	20110	1?110	?1?
Anserimimus	?????	?????	?????	???11	10100	21211	01100	111
Gallimimus	11111	11111	11100	00111	111(01)1	2(01)111	11100	111
Struthiomimus	11110	01?11	11110	11111	01001	?0111	11101	111
Dromiceiomimus	1111?	11?11	1??10	1???1	00011	10???	??101	111
Ornithomimus	11110	11?11	11111	11111	00011	20211	11101	111
Sinornithomimus	11111	11111	111?0	1?111	0(01)011	20110	11100	111